that the chromatin reorganization related to the transcriptional regulation occurred in spatiotemporally-specific manner and is supported by a number of specific protein complexes (Ju *et al.* 2006; Garcia-Bassets *et al.* 2007). Moreover, specific combinations of the complex components appear to be highly regulated responding to extracellular signals. Redox condition is presumed as such a key determinant, and affects the biological conditions affecting the cell fate. Although it is generally accepted that redox condition modulates the property of transcription factors, it remains to be understood how it regulates the conditions of promoter regions around the target gene promoters of transcription factors, particularly in terms of complex formation (Pouyssegur & Mechta-Grigoriou 2006).

Three types of redox state-dependent transcriptional regulation have been described so far. One is a direct oxidation/reduction of cysteines on the transcription factor itself (e.g. AP-1). The second is a change of the factor's subcellular localization as in the case of NF-κB. The last are alterations of the redox buffers (e.g. NAD^+/NADH exchange) which change the properties of transcriptional repressors such as CtBP or SirT1 (Zhang *et al.* 2002; Liu *et al.* 2005). In this study using the GR, we found a novel mechanism of redox-dependent transcriptional regulation (Tanaka *et al.* 2000). In this model, blockade of GR protein degradation by the deoxiding agent $CoCl_2$ increased co-factor recruitment and consequently potentiates the GR transactivation property. We used a representative GR interacting co-factor Brg-1, an ATP-dependent chromatin remodeling factor, as an example of co-factor recruitment in our experiments. We also presume that various types of co-factor complexes may be associated with GR at different timing after redox stimulus. A detailed time course analysis is essential to completely understand this form of redox-dependent transcriptional regulation. Moreover, further extensive biochemical analysis is needed to fully describe how the regulation of protein stabilization affects the transcriptional regulation of various nuclear receptors in different biological situations (Lonard & O'Malley 2006; Ohtake *et al.* 2007).

Regarding the redox–dependent regulation of GR transcriptional function, another regulatory mechanism has already been reported in a certain cell line (Leonard *et al.* 2005). However, such up-regulation of GR mRNA levels by hypoxia was not observed in the tested cell lines in the present study. Such regulatory mechanisms by hypoxia as well as reduction state may be diverse and may appear in cell context-dependent manner.

It is well known that some nuclear receptors including the GR have an anti-inflammatory effect resulting from the repression of AP-1 or NF-κB mediated transcription in ligand-dependent manner (Smoak & Cidlowski 2004; Valledor & Ricote 2004). The mechanism for this form of transrepression is largely unknown (Ogawa *et al.* 2005; Reily *et al.* 2006). Additionally, increasing co-factor (Brg-1) recruitment on target gene promoters by receptor protein stabilization was not sufficient to potentate the transrepressional property of the GR in the reduced state (see Figs 1 and 3B). These results suggest that distinct co-regulators or protein modifications may affect these transrepressional mechanisms (Kodama *et al.* 2003). To investigate this further, we are establishing a biochemical purification system for analyzing GR transcriptional regulation under various conditions.

Experimental procedures

Reagents and plasmids

Plasmids

The full-length human GR was inserted into the pNTAP expression vector using the InterPlay™ Mammalian TAP system (Stratagene, Cedar Creek, TX). It was also inserted into the pEGFP-C2 vector (BD Bioscience, San Jose, CA). Human GR mutants (Cys 481 for Ser) for both vectors were made with the QuikChange site-directed mutagenesis kit (Stratagene). pGRE-Luc was purchased from BD Bioscience. pAP1-Luc and pNF-κB-Luc were purchased from Stratagene. Expression vectors with c-Jun, c-Fos, p50 and p65 were cloned from a 293T cDNA library and inserted into the pcDNA3 vector (Invitrogen, Carlsbad, CA).

Antibodies

Anti-human GR antibody (PA1–512) was purchased from Affinity BioReagents (ABR, Golden, CO). Anti-Brg-1 Antibody (H-88) and β-actin (I-19) was purchased from Santa Cruz Biotechnology, Inc. (Santa Cruz, CA).

Reagents

Dexamethasone was purchased from Sigma (St. Louis, MO). H_2O_2 and $CoCl_2$ were purchased from Wako Chemicals, and MG132 was purchased from Peptide Institute Inc (Osaka, Japan).

Reporter assay

293F cells were transfected using the Lipofectamine Plus reagent (Invitrogen) according to the manufacturer's protocol. Luciferase reporter plasmids were co-transfected with the GR-expression vectors as indicated in the figure legends together with 2 ng/well of pRL-CMV plasmid (Promega, Madison, WI). After 3 h of transfection, the media were replaced with fresh media containing 0.2% fetal bovine serum. Dexamethasone (10^{-7} M), H_2O_2 (0.1 mM) or $CoCl_2$ (0.2 mM) were then added to the cells and incubated for an additional 12 h. Cell extract preparation and dual luciferase assays were performed according to the manufacturer's

protocols (Promega). Individual transfections performed in triplicate wells were repeated at least 3 times.

Preparation of stably transfected cell lines

TAP-tagged human GR-expressing retroviruses were produced using a pQCXIN vector (BD Bioscience). The 293F cells were infected by incubating them with the virus and 6 μg/mL hexadimethrine bromide (Sigma). Cells stably expressing the GR were combined and cultured with 700 μg/mL G418 (Promega) prior to colony selection.

RNA extraction and RT-PCR

Total cellular RNA was isolated from A549 cells by ISOGEN (Wako). RT reaction was performed using SuperScript (Invitrogen) and the indicated mRNAs were amplified by PCR as previously reported (Kitagawa *et al.* 2003).

Immunoprecipitation and Western blotting

After treating 293F cells or A549 cells with either H_2O_2 or $CoCl_2$ for the indicated time, cells were washed twice with ice-cold phosphate-buffered saline, resuspended in 1 mL ice-cold lysis buffer [10 mM Tris–HCl (pH 4.7), 10 mM NaCl, 3 mM $MgCl_2$, 0.5% (vol/vol) NP-40] and incubated on ice for 30 min. Cells were then centrifuged again for 5 min at 500*g* and the sedimented nuclear fractions resuspended in TNE buffer [10 mM Tris–HCl (pH 7.5), 0.15 M NaCl, 1 mM EDTA, 1% NP-40] and incubated for 30 min on ice. After centrifugation, supernatants were used as cell extracts for immunoprecipitation using anti-GR antibody with protein G Sepharose and then Western blotted with an anti-GR polyclonal antibody or anti-Brg-1 antibody.

ChIP assay

Soluble chromatin from A549 cells was prepared with the acetyl-histone H4 immunoprecipitation assay kit (Upstate Biotechnology, Billerica, MA) and was immunoprecipitated with antibodies against the indicated proteins (Kitagawa *et al.* 2003). Specific primer pairs were designed to amplify the promoter region of human αENAC (5′-TTCCTTTCCAGCGCTGGCCAC-3′ and 5′-CCTCCAACCTTGTCCAGACCC-3′), human collagenase 1 (5′-GCAGAGTGTGTCTCTTTCGCACAC-3′ and 5′-GCCCTTCCAGAAAGCCAGAGGCTG-3′), human IL-8 (5′-GGGCCATCAGTTGCAAATC-3′ and 5′-TTCCT-TCCGGTGGTTTCTTC-3′) from genomic DNA (Kitagawa *et al.* 2002; Kassel *et al.* 2004). PCR conditions were optimized to allow semi-quantitative measurement and PCR products were visualized on 2% agarose/TAE gels.

Acknowledgements

We thank Dr S. Kido, and T. Matsumoto in Tokushima University for plasmid transferring. Also we thank Ms Hiraga for manuscript handling.

References

Dennis, A.P. & O'Malley, B.W. (2005) Rush hour at the promoter: how the ubiquitin-proteasome pathway polices the traffic flow of nuclear receptor-dependent transcription. *J. Steroid Biochem. Mol. Biol.* **93**, 139–151.

Garcia-Bassets, I., Kwon, Y.S., Telese, F., Prefontaine, G.G., Hutt, K.R., Cheng, C.S., Ju, B.G., Ohgi, K.A., Wang, J., Escoubet-Lozach, L., Rose, D.W., Glass, C.K., Fu, X.D. & Rosenfeld, M.G. (2007) Histone methylation-dependent mechanisms impose ligand dependency for gene activation by nuclear receptors. *Cell* **128**, 505–518.

Garside, H., Waters, C., Berry, A., Rice, L., Ardley, H.C., White, A., Robinson, P.A. & Ray, D. (2006) UbcH7 interacts with the glucocorticoid receptor and mediates receptor autoregulation. *J. Endocrinol.* **190**, 621–629.

Heck, S., Kullmann, M., Gast, A., Ponta, H., Rahmsdorf, H.J., Herrlich, P. & Cato, A.C. (1994) A distinct modulating domain in glucocorticoid receptor monomers in the repression of activity of the transcription factor AP-1. *EMBO J.* **13**, 4087–4095.

Jonat, C., Rahmsdorf, H.J., Park, K.K., Cato, A.C., Gebel, S., Ponta, H. & Herrlich, P. (1990) Antitumor promotion and antiinflammation: down-modulation of AP-1 (Fos/Jun) activity by glucocorticoid hormone. *Cell* **62**, 1189–1204.

Ju, B.G., Lunyak, V.V., Perissi, V., Garcia-Bassets, I., Rose, D.W., Glass, C.K. & Rosenfeld, M.G. (2006) A topoisomerase IIβ-mediated dsDNA break required for regulated transcription. *Science* **312**, 1798–1802.

Kassel, O., Schneider, S., Heilbock, C., Litfin, M., Gottlicher, M. & Herrlich, P. (2004) A nuclear isoform of the focal adhesion LIM-domain protein Trip6 integrates activating and repressing signals at AP-1- and NF-κB-regulated promoters. *Genes Dev.* **18**, 2518–2528.

Kim, H.J., Jung, K.J., Yu, B.P., Cho, C.G., Choi, J.S. & Chung, H.Y. (2002) Modulation of redox-sensitive transcription factors by calorie restriction during aging. *Mech. Ageing Dev.* **123**, 1589–1595.

Kishimoto, M., Fujiki, R., Takezawa, S., Sasaki, Y., Nakamura, T., Yamaoka, K., Kitagawa, H. & Kato, S. (2006) Nuclear receptor mediated gene regulation through chromatin remodeling and histone modifications. *Endocr. J.* **53**, 157–172.

Kitagawa, H., Fujiki, R., Yoshimura, K., *et al.* (2003) The chromatin-remodeling complex WINAC targets a nuclear receptor to promoters and is impaired in Williams syndrome. *Cell* **113**, 905–917.

Kitagawa, H., Yanagisawa, J., Fuse, H., Ogawa, S., Yogiashi, Y., Okuno, A., Nagasawa, H., Nakajima, T., Matsumoto, T. & Kato, S. (2002) Ligand-selective potentiation of rat mineralocorticoid receptor activation function 1 by a CBP-containing histone acetyltransferase complex. *Mol. Cell. Biol.* **22**, 3698–3706.

Kodama, T., Shimizu, N., Yoshikawa, N., Makino, Y., Ouchida, R., Okamoto, K., Hisada, T., Nakamura, H., Morimoto, C. & Tanaka, H. (2003) Role of the glucocorticoid receptor for regulation of hypoxia-dependent gene expression. *J. Biol. Chem.* **278**, 33384–33391.

Kumar, R., Wang, R.A. & Barnes, C.J. (2004) Coregulators and chromatin remodeling in transcriptional control. *Mol. Carcinog.* **41**, 221–230.

Leonard, M.O., Godson, C., Brady, H.R. & Taylor, C.T. (2005) Poteintiation of glucocorticoid activity in hypoxia through induction of the glucocorticoid receptor. *J. Immunol.* **174**, 2250–2256.

Liu, H., Colavitti, R., Rovira, II & Finkel, T. (2005) Redox-dependent transcriptional regulation. *Circ. Res.* **97**, 967–974.

Lonard, D.M. & O'Malley, B.W. (2006) The expanding cosmos of nuclear receptor coactivators. *Cell* **125**, 411–414.

Miyamoto, J., Matsumoto, T., Shiina, H., Inoue, K., Takada, I., Ito, S., Itoh, J., Minematsu, T., Sato, T., Yanase, T., Nawata, H., Osamura, Y.R. & Kato, S. (2007) The pituitary function of androgen receptor constitutes a glucocorticoid production circuit. *Mol. Cell. Biol.* **27**, 4807–4814.

Nagaich, A.K., Walker, D.A., Wolford, R. & Hager, G.L. (2004) Rapid periodic binding and displacement of the glucocorticoid receptor during chromatin remodeling. *Mol. Cell* **14**, 163–174.

Ogawa, S., Lozach, J., Benner, C., Pascual, G., Tangirala, R.K., Westin, S., Hoffmann, A., Subramaniam, S., David, M., Rosenfeld, M.G. & Glass, C.K. (2005) Molecular determinants of crosstalk between nuclear receptors and toll-like receptors. *Cell* **122**, 707–721.

Ohtake, F., Baba, A., Takada, I., Okada, M., Iwasaki, K., Miki, H., Takahashi, S., Kouzmenko, A., Nohara, K., Chiba, T., Fujii-Kuriyama, Y. & Kato, S. (2007) Dioxin receptor is a ligand-dependent E3 ubiquitin ligase. *Nature* **446**, 562–566.

Okamoto, K., Tanaka, H., Ogawa, H., Makino, Y., Eguchi, H., Hayashi, S., Yoshikawa, N., Poellinger, L., Umesono, K. & Makino, I. (1999) Redox-dependent regulation of nuclear import of the glucocorticoid receptor. *J. Biol. Chem.* **274**, 10363–10371.

Perissi, V. & Rosenfeld, M.G. (2005) Controlling nuclear receptors: the circular logic of cofactor cycles. *Nat. Rev. Mol. Cell Biol.* **6**, 542–554.

Pouyssegur, J. & Mechta-Grigoriou, F. (2006) Redox regulation of the hypoxia-inducible factor. *Biol. Chem.* **387**, 1337–1346.

Qiu, Y., Zhao, Y., Becker, M., *et al.* (2006) HDAC1 acetylation is linked to progressive modulation of steroid receptor-induced gene transcription. *Mol. Cell* **22**, 669–679.

Rahman, I., Biswas, S.K. & Kirkham, P.A. (2006) Regulation of inflammation and redox signaling by dietary polyphenols. *Biochem. Pharmacol.* **72**, 1439–1452.

Rahman, I., Marwick, J. & Kirkham, P. (2004) Redox modulation of chromatin remodeling: impact on histone acetylation and deacetylation, NF-κB and pro-inflammatory gene expression. *Biochem. Pharmacol.* **68**, 1255–1267.

Reily, M.M., Pantoja, C., Hu, X., Chinenov, Y. & Rogatsky, I. (2006) The GRIP1 × IRF3 interaction as a target for glucocorticoid receptor-mediated immunosuppression. *EMBO J.* **25**, 108–117.

Rhen, T. & Cidlowski, J.A. (2005) Antiinflammatory action of glucocorticoids—new mechanisms for old drugs. *N. Engl. J. Med.* **353**, 1711–1723.

Rogatsky, I. & Ivashkiv, L.B. (2006) Glucocorticoid modulation of cytokine signaling. *Tissue Antigens* **68**, 1–12.

Rosenfeld, M.G., Lunyak, V.V. & Glass, C.K. (2006) Sensors and signals: a coactivator/corepressor/epigenetic code for integrating signal-dependent programs of transcriptional response. *Genes Dev.* **20**, 1405–1428.

Saklatvala, J. (2002) Glucocorticoids: do we know how they work? *Arthritis. Res.* **4**, 146–150.

Smoak, K.A. & Cidlowski, J.A. (2004) Mechanisms of glucocorticoid receptor signaling during inflammation. *Mech. Ageing Dev.* **125**, 697–706.

Takezawa, S., Yokoyama, A., Okada, M., Fujiki, R., Iriyama, A., Yanagi, Y., Ito, H., Takada, I., Kishimoto, M., Miyajima, A., Takeyama, K., Umesono, K., Kitagawa, H. & Kato, S. (2007) A cell cycle-dependent co-repressor mediates photoreceptor cell-specific nuclear receptor function. *EMBO J.* **26**, 764–774.

Tanaka, H., Makino, Y., Okamoto, K., Iida, T., Yoshikawa, N. & Miura, T. (2000) Redox regulation of the nuclear receptor. *Oncology* **59** Suppl 1, 13–18.

Valledor, A.F. & Ricote, M. (2004) Nuclear receptor signaling in macrophages. *Biochem. Pharmacol.* **67**, 201–212.

Wang, J.C., Derynck, M.K., Nonaka, D.F., Khodabakhsh, D.B., Haqq, C. & Yamamoto, K.R. (2004) Chromatin immunoprecipitation (ChIP) scanning identifies primary glucocorticoid receptor target genes. *Proc. Natl. Acad. Sci. USA* **101**, 15603–15608.

Yanagisawa, J., Kitagawa, H., Yanagida, M., Wada, O., Ogawa, S., Nakagomi, M., Oishi, H., Yamamoto, Y., Nagasawa, H., McMahon, S.B., Cole, M.D., Tora, L., Takahashi, N. & Kato, S. (2002) Nuclear receptor function requires a TFTC-type histone acetyl transferase complex. *Mol. Cell* **9**, 553–562.

Zhang, Q., Piston, D.W. & Goodman, R.H. (2002) Regulation of corepressor function by nuclear NADH. *Science* **295**, 1895–1897.

Received: 11 June 2007
Accepted: 10 August 2007

Available online at www.sciencedirect.com
ScienceDirect
Archives of Biochemistry and Biophysics 460 (2007) 166–171
ABB
www.elsevier.com/locate/yabbi

Multiple co-activator complexes support ligand-induced transactivation function of VDR

Kazuyoshi Yamaoka [b], Masayo Shindo [a], Kei Iwasaki [b], Ikuko Yamaoka [b], Yoko Yamamoto [a], Hirochika Kitagawa [a], Shigeaki Kato [a,b,*]

[a] *Institute of Molecular and Cellular Biosciences, University of Tokyo, 1-1-1 Yayoi, Bunkyo-ku, Tokyo 113-0032, Japan*
[b] *ERATO, Japan Science and Technology Agency, 4-1-8 Honcho, Kawaguchisi, Saitama 332-0012, Japan*

Received 20 June 2006, and in revised form 26 July 2006
Available online 14 August 2006

Abstract

Vitamin D receptor (VDR) mediates a wide variety of vitamin D actions through transcriptional controls of target genes as a ligand-dependent transcription factor. The transactivation by VDR is known to associate with two co-activator complexes, DRIP/TRAP and p160/CBP, through physical interaction with DRIP205 and p160 members (TIF2) components, respectively. However, functional difference between the two co-activator complexes for VDR co-activation remains unclear. In the present study, to address this issue, a series of point mutants in VDR helix 12 were generated to test the functional association. Alanine replacement of VDR valine 418 resulted in loss of DRIP205 interaction, but it was still transcriptionally potent with ability to interact with TIF2. Surprisingly, the V421A mutant was only partially impaired in transactivation without co-activator interaction, implying presence of a putative co-activator/complex. Thus, these findings suggest that ligand-induced transcriptional controls by VDR require a number of known and unknown co-regulator complexes, that may support the tissue-specific function of VDR.

Keywords: Vitamin D; Vitamin D receptor; Co-activator; Co-regulator complex; Ligand-induced transactivation; Helix 12; Vitamin D 24-hydroxylase

Calciotropic hormone 1, $25(OH)_2D_3$, the active form of vitamin D_3, regulates calcium homeostasis as well as cellular proliferation and differentiation [1]. Most biological actions of 1, $25(OH)_2D_3$ are believed to be mediated through transcriptional control of a particular set of target genes by the vitamin D receptor (VDR)[1] [2,3]. The VDR is a member of the nuclear receptor (NR) gene superfamily, and acts as a ligand-inducible transcription factor by heterodimerizing with another NR member, RXR [4]. Like other members of the NR superfamily, VDR structure is divided into several functional domains. The most highly conserved DNA binding domain (C) is located centrally whilst the less highly conserved ligand binding domain (E) is located at the C-terminal end [5]. Most nuclear receptors harbor both N-terminal activation function 1 (AF-1) and C-terminal AF-2 domains [6]. However, the VDR appears to lack the significant N-terminal AF-1 function due to its relatively short A/B domain.

In the promoters of target genes, VDR/RXR heterodimers recognize and directly bind to cognate vitamin D responsive elements (VDREs) [6], following recruitment of a number of co-regulators and co-regulatory complexes. Such co-regulators and complexes appear to transiently associate with VDR, and their recruitment is considered to be highly regulated and cyclic among the complexes [7]. A group of co-regulator complexes that normally form large complexes with multiple components and support ligand-dependent transcriptional control of NRs have been identified, and have been classified into three categories according to their function [8]. The major function of the first class of

* Corresponding author. Fax: +81 3 5841 8477.
E-mail address: uskato@mail.ecc.u-tokyo.ac.jp (S. Kato).

[1] *Abbreviations used:* VDR, vitamin D receptor; NR, nuclear receptor; AF-1, activation function 1; VDREs, vitamin D responsive elements; HAT, histone acetyltransferase.

0003-9861/$ - see front matter © 2006 Elsevier Inc. All rights reserved.
doi:10.1016/j.abb.2006.07.015

complexes is chromatin remodeling, which involves the ATP-dependent dynamic remodeling of chromatin structure [9–13]. Chromatin remodeling complexes utilize energy from ATP hydrolysis to rearrange nucleosomal arrays in a non-covalent manner. For VDR, a specific ATP-dependent chromatin remodeling complex, WINAC, has been biochemically identified [11]. A second co-regulator complex class regulates transcriptional control directly, through physical interaction with general transcription factors and RNA polymerase II [14,15]. The DRIP/TRAP co-activator complex has been well-described as a representative of this complex class to co-activate liganded NRs in vivo and in vitro.

Members of a third co-regulator complex class are classified to modify histone tails covalently, for example, by acetylation, methylation and phosphorylation, in promoter nucleosomal arrays [16–19]. p160 family members/p300/CBP histone acetylase (HAT) co-activator complex has been well characterized as a typical member of this class. This type of HAT co-activator complex harbors one of three p160 HAT family members (SRC-1 [18], TIF2 [20,21], AIB1 [22–26]) and one of CBP/p300 HAT [27] together with other components. In addition of such co-regulator complexes to define histone acetylation state, the other histone modifying enzyme complexes to methylate histones appear to support the ligand-dependent transcriptional activation by NRs [28,29]. Though the DRIP/TRAP non-HAT and the p160/CBP HAT complexes have been described to co-activate VDR [7,30], it remains to be addressed if the other histone modifying enzyme complexes are required for VDR transactivation.

Ligand-dependent interaction of NRs with co-activator complexes are mediated through physical interaction of consensus LXXLL and related motifs present on specific complex components and the C-terminal helix 12 (H12) of the NR LBD domain [31]. The ligand-induced association of NRs with complexes is stabilized by ligand binding-induced shifting of NR H12. The molecular basis of this ligand-induced association has been deduced by X-ray analysis [32,33].

Considering the tissue-specific gene regulation by VDR from a variety of phenotypic abnormalities seen in VDR KO mice [34], the present study was undertaken to examine whether VDR requires multiple types of transcriptional co-regulator complexes. To address this issue, we generated a series of VDR H12 mutants and tested co-activation of the VDR mutants by two classes of different co-activator complexes (DRIP/TRAP and p160/CBP complexes). A VDR H12-point mutant, that selectively lost its ability to physically interact with the TRAP/DRIP complex, was still potent in ligand-induced transactivation. Another VDR H12-point mutant, that was unable to associate with either co-activator in vitro, still retained ligand-induced transactivation. Thus, taken together, our results suggest that multiple known and unknown types of co-activator complex support ligand-induced transactivation by VDR.

Material and methods

Materials

Rat VDR cDNA in pSG5 [30] was applied to generate a series of alanine point replaced mutants in the VDR H12. Mutagenesis was performed through PCR with specific sets of oligonucleotide primers. For GST fusion proteins of the VDR point mutants, the cDNAs of VDR LBD point mutants were inserted into pGEX-4T-1. For one-hybrid analysis of the VDR mutants with TIF2, TIF2 cDNA was fused with a cDNA of VP16 activation domain to generate a TIF2 chimeric protein with VP16.

Cell culture and transient transfection

COS-1 cells (derived from monkey kidney) and 293T cells (derived from human kidney) were maintained in DMEM supplemented with 5% FBS (Gibco) at 37 °C, 5% CO_2. For transfection, cells were cultured in DMEM (phenol red-free) supplemented with 5% charcoal-stripped FBS. Cells were transfected with expression vectors of either VDR, RXR, co-activators, or the combined and were harvested for 24 h, after treatment with vehicle or 1, $25(OH)_2D_3$ (1×10^{-8} M). For one-hybrid analysis, the expression vectors of VDR mutants and VP16-TIF2 chimeric protein were transfected and incubated for 24 h in the presence of 1, $25(OH)_2D_3$ (1×10^{-8} M). The total cell extracts prepared from the transfectants were applied for a luciferase assays as described [11].

Western blotting

The transfected COS-1 cells used for the luciferase assay were also utilized for Western blotting analysis to measure the expression levels of the VDR mutants. Briefly the transfectants were lysed in TNE (10 mM Tris–HCl, pH 7.8, 1% Nonidet P-40, 0.15 M NaCl, 1 mM EDTA, 1 mM phenylmethylsulfonyl fluoride, 1 μg/ml aprotini) buffer. Cell lysates were separated by 8% SDS–polyacrylamide gel eletrophoresis, transferred onto polyvinylidene difluoride membranes (Milliopore) and detected with rat anti-VDR monoclonal antibody (NeoMarkers) and anti-rat IgG antibody conjugated with horseradish peroxidase (Dako).

GST pull-down assay

For the GST pull-down assay, TIF2 and DRIP205 were in vitro-translated and incubated with GST-fused a series of VDR point mutants deleting the A/B and C domain as illustrated in Fig. 3, immobilized on glutathione–Sepharose beads, in the absence or presence of 1, $25(OH)_2D_3$ (1×10^{-6} M) [35].

Chromatin immunoprecipitation

Soluble chromatin from 293T cells derived from human kidney, prepared using the chromatin immunoprecipitation assay kit (Upstate), was immunoprecipitated with antibodies against the indicated proteins [11,36]. Specific primer pairs were designed to amplify the promoter region of human vitamin D 24 hydroxylase (5′-GGGAGGCGCGTTCGAA-3′ and 5′-TCCTATGCCCAGGGAC-3′), from genomic DNA. PCR conditions were optimized to allow semi-quantitative measurement and PCR products were visualized on 2% agarose/TAE gels.

Results

Several, but not all, point mutations in VDR helix 12 impair ligand-induced transactivation function

As illustrated in Fig. 1, a series of alanine replacements were introduced into the transactivation core domain (AD core) in the VDR H12 domain. The amino acid

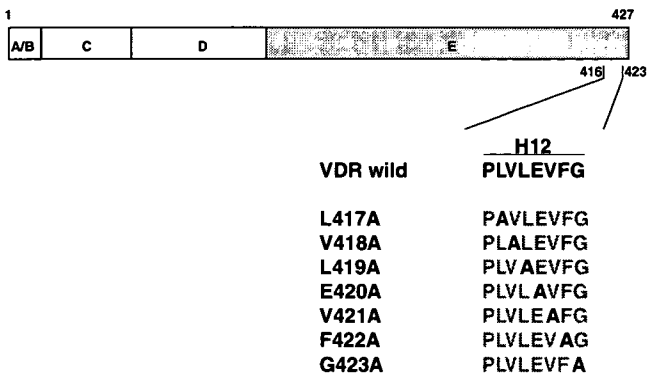

Fig. 1. Schematic representation of VDR point mutants. Rat VDR protein is schematically displayed, and alanine point replacement in H12 domains are indicated in the lower panel.

residue number of rat VDR H12 is adjusted to those of human VDR, since the length and amino acid residues of H12 is identical between rat and human. We then examined the ligand-induced transactivation function of the VDR mutants by a transient expression assay with their expression vectors and a luciferase reporter plasmid containing a consensus VDRE (DR3) in its promoter. The plasmids were transfected with a renal cell line, COS-1 cells as indicated in Fig. 2.

Ligand-induced transactivation of VDR in the presence of RXR was severely impaired by alanine replacement at 417Leu, 420Glu, 422Phe, while only partial reductions in transactivation were observed in V418A, L419A and V421A VDR H12 mutants. Unexpectedly, the 423 glycine replacement (G423A) rather potentiated ligand-induced transactivation of VDR. Thus, the loss of ligand-induced transactivation of 417, 420 and 422 VDR point mutations was expected to be caused by abrogation of co-activator interaction through H12. In contrast, the

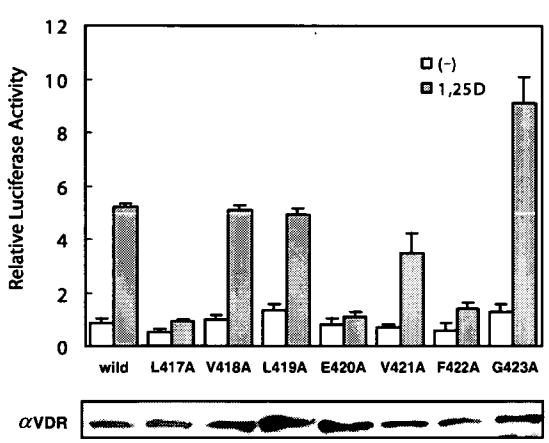

Fig. 2. H12 point mutations of VDR caused altered transactivation function of liganded VDR. The expression vectors of VDR mutants were transfected with COS-1 cells in the presence of 1, 25$(OH)_2D_3$ (1×10^{-8} M). The transfected cells were applied for a luciferase analysis. The averages of the results from three independent experiments are shown with ±SD (upper panel). The expression levels of the VDR mutants were verified by Western blotting with a specific antibody for VDR (lower panel).

retained though diminished activities of the other mutants suggest there was still a retained ability to interact with co-activators in a ligand-dependent manner in some mutants. The transcriptional activities of the VDR mutants appeared unlikely due to the mutant expression levels, when the expression levels were estimated by Western blot analysis (see lower panel in Fig. 2). Note that we could confirm the same observations in human kidney cell line 293T cells (data not shown).

Different usage of co-activators for VDR H12-point mutants

To verify whether transcriptionally active VDR H12 mutants are capable of interacting with the best characterized co-activators, ligand-induced interaction of VDR mutants with DRIP205/TRAP220 and TIF2 co-activators was tested. DRIP205/TRAP220 was originally identified to physically interact in vitro with liganded VDR as a non-HAT DRIP/TRAP co-activator complex component. This complex then co-activated VDR as observed by an in vitro transcription assay [15]. TIF2, one of three p160 HAT co-activator family members, has been well described to associate with VDR in a ligand-dependent manner. By a GST pull-down assay, the inactive VDR mutants (L417A, E420A and F422A) were expectedly seen to lose their co-activator interactions (Fig. 3). Surprisingly, a transcriptionally active VDR mutant (V421A) was also unable to associate with either co-activator, and the V418A mutant interacted with only TIF2, but not DRIP205. To confirm these observations, a one-hybrid system with the VDR mutants and a TIF2 chimeric protein fused with a VP16 activation domain for a sensitive detection, was used to detect ligand-induced interaction of the VDR mutants with TIF2. Reflecting the observation in vitro, TIF2 interactions were observed in the V418A, L419A, and G423A mutants, but not in the V421A mutant in COS-1 cells (Fig. 4) and 293T cells (data not shown).

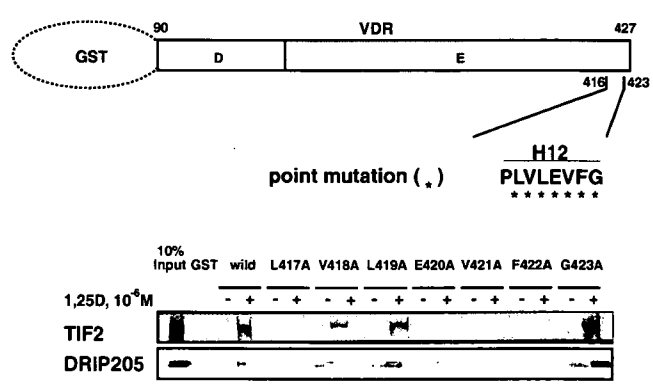

Fig. 3. Differential associations of VDR mutants with co-activators. Singular print mutations (*) introduced into H12 in the GST-VDR were the same as shown in Fig. 1. Two best known co-activators (TIF2 and DRIP205) were in vitro translated and incubated with the bacterially expressed VDR chimeric mutants fused with GST in the absence (−) or presence (+) of 1, 25$(OH)_2D_3$ (1×10^{-6} M). The association was visualized on SDS–PAGE.

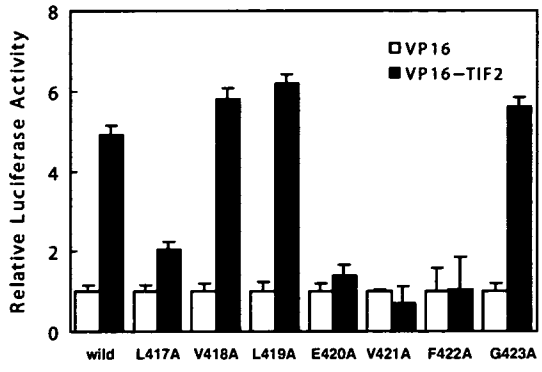

Fig. 4. The V421A VDR mutant failed to functionally associate with TIF2. As described in Fig. 2, a luciferase assay was performed for one-hybrid assay to detect ligand-dependent association of the VDR mutants with TIF2. Although V421A mutant was only partially impaired in the ligand-induced transactivation, this mutant failed to interact with TIF2, in accordance with in vitro GST-pull down assay (see Fig. 3).

VDR H12 mutants are recruited to the target promoter in vivo

We could not still exclude the possibility that several H12 point-mutations disable VDR from associating with the target promoter, leading to impaired transactivation in the transient expression assay, even though the expression levels of the VDR mutants were unaltered by the point mutations. To address this issue, we tested if these mutants are recruited to the endogenous target promoter of human vitamin D 24 hydroxylase [24(OH)ase] gene, that is well known to contain typical VDRE [37] by ChIP analysis. As shown in Fig. 5, V418A and V421A were recruited to the promoters, and the transcriptionally inactive VDR mutants were also recruited (data not shown). These findings clearly suggest that promoter targeting of VDR/RXR heterodimer to the target promoter does not directly couple with transactivation function of liganded VDR. As the HAT co-activators recruited to ligand VDR are presumed to acetylate histones for histone modification, histone modification may be dispensable for promoter targeting of VDR.

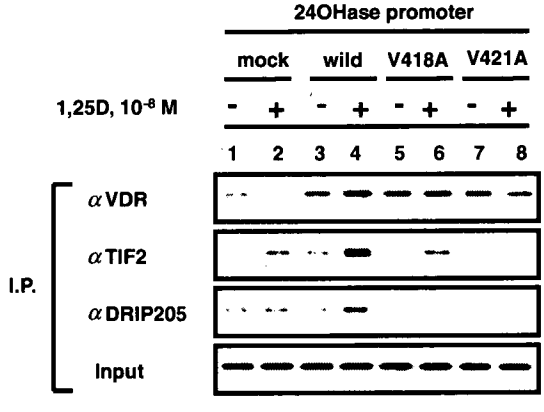

Fig. 5. The VDR point mutants were recruited to the human vitamin D 24-hydroxylase gene promoter. ChIP analysis was performed in the human vitamin D 24-hydroxylase gene promoter in 293T cells transfected with the indicated plasmids shown in the figure. The immobilized chromatin immunoprecipitated by a specific antibody was used for PCR to detect the factor bindings as described in Materials and methods.

Discussion

Is chromatin remodeling and histone modification independent from VDR-mediated gene regulation?

In our study, we have already reported that ligand-induced transactivation and transrepression mediated VDR requires chromatin remodeling through one class of ATP-dependent chromatin remodeling complex, WINAC [11,38]. Ligand-independent association of VDR with WSTF protein in the WINAC complex as well as non-specific but significant interaction of the WSTF bromo domain with acetylated histone appear to assist targeting of VDR to specific DNA binding regions in the VDR target gene promoters [38]. At the present time it is unclear whether chromatin remodeling is coupled with histone modification in VDR-mediated gene regulations. For sex steroid hormone receptors, histone modification appears indispensable prior to chromatin remodeling since steroid receptor recruitment to the target promoter is dependent on ligand binding [39]. This is presumably accompanied by recruitment of histone modifying enzyme co-regulator complexes that undergo histone modification. However, unlike steroid receptors, we observed ligand-independent recruitment of VDR to the target promoters, implying a possibility that promoter targeting of VDR does not require histone modification. This idea was further supported by the observations that the V421A VDR H12 mutant is unable to associate with the p160 HAT co-activators, but was still recruited to the promoter (Fig. 5). Thus, it is more likely that WINAC associating with VDR remodels the target chromosomal areas to expose VDREs, leading to stable DNA binding of VDR/RXR.

The two classes of co-activator have distinct sites of direct contact with VDR AF-2

By generating a series of VDR mutants, we have shown in this study that point-mutations in VDR H12 regions result in loss of ligand binding-dependent ability to associate with the tested co-activators, DRIP205 and TIF2. This would agree with the recent view that H12 serves as a direct interface for co-activator interaction through physical interaction with LXXLL motifs of the co-activators [40,41]. By detailed analysis of the interaction of VDR H12 mutants with co-activators in vitro, we found that a VDR H12 mutant (V418A) lacking ligand-induced ability to associate with DRIP205 is still capable of interacting with the other class of co-activator TIF2 (Figs. 3 and 4). These findings were unexpected, since the H12 domain is well established to serve as the direct interface to recruit DRIP205 in the DRIP/TRAP co-activator complex [42]. Indeed, loss of the interaction with DRIP205 was also confirmed to impair ligand-induced transactivation of VDR in vitro. As this V418A mutant was still transcriptionally ligand-inducible, this mutation appears unlikely to abrogate the indispensable H12 property of ligand-induced H12

shifting. Moreover, ligand-induced recruitment to VDR was seen in the VDR target gene promoter by ChIP analysis (Fig. 5). Thus, together with these findings, it is most likely that ligand-induced transactivation of VDR is supported by multiple classes of co-activator complex.

A third co-activator complex for VDR?

Accumulating evidence of co-regulator/co-regulator complex identification suggests that ligand-induced transactivation of nuclear receptors is supported by a number of co-regulators/co-regulator complexes [43,44]. Each co-regulators complex is believed to govern a distinct process in gene regulation.

However, at least among co-activators, functional redundancy is observed in our in vitro transactivation assays. In the present study, the V421A VDR H12 mutant was unexpectedly transcriptionally active even though this mutant lost its ability to interact with either class of co-activator complexes, both of which have been shown indispensable for ligand-induced transactivation of VDR in vitro [12,14,15]. These findings indicate the possible existence of other co-activator complexes. Although histone acetylation is well described to trigger chromatin activation for following gene expression, methylation of specific residues of histone tails has recently proposed to also enable chromatin active for transcription [28,29]. In this respect, like the other NR members, histone methylase complex(es) recruited to liganded VDR may be potent enough to activate chromatin through functional association with HAT complexes, leading co-activation of liganded VDR. To verify this idea, identification of the third critical co-activator/co-activator complex using several distinct approaches is required. Such studies would enhance our understanding of the spatial and temporal function of VDR in various target tissues.

Acknowledgments

We thank Teijin Pharma Ltd. for the 1α, $25(OH)_2D_3$. We also thank H. Higuchi for manuscript preparation. This work was supported in part by the Program for Promotion of Basic Research Activities for Innovative Biosciences (PROBRAIN) and priority areas from the Ministry of Education, Culture, Sports, Science and Technology (to S.K.).

References

[1] H.F. DeLuca, Adv. Exp. Med. Biol. 196 (1986) 361–375.
[2] R. Bouillon, W.H. Okamura, A.W. Norman, Endocr. Rev. 16 (1995) 200–257.
[3] M.R. Walters, Endocr. Rev. 13 (1992) 719–764.
[4] D.J. Mangelsdorf, C. Thummel, M. Beato, P. Herrlich, G. Schutz, K. Umesono, B. Blumberg, P. Kastner, M. Mark, P. Chambon, R.M. Evans, Cell 83 (1995) 835–839.
[5] M.R. Hughes, P.J. Malloy, D.G. Kieback, R.A. Kesterson, J.W. Pike, D. Feldman, B.W. O'Malley, Science 242 (1988) 1702–1705.
[6] M.R. Haussler, G.K. Whitfield, C.A. Haussler, J.C. Hsieh, P.D. Thompson, S.H. Selznick, C.E. Dominguez, P.W. Jurutka, J. Bone Miner. Res. 13 (1998) 325–349.
[7] S. Kim, N.K. Shevde, J.W. Pike, J. Bone Miner. Res. 20 (2005) 305–317.
[8] C.K. Glass, M.G. Rosenfeld, Genes Dev. 14 (2000) 121–141.
[9] D.V. Fyodorov, J.T. Kadonaga, Cell 106 (2001) 523–525.
[10] T. Ito, M. Bulger, M.J. Pazin, R. Kobayashi, J.T. Kadonaga, Cell 90 (1997) 145–155.
[11] H. Kitagawa, R. Fujiki, K. Yoshimura, Y. Mezaki, Y. Uematsu, D. Matsui, S. Ogawa, K. Unno, M. Okubo, A. Tokita, T. Nakagawa, T. Ito, Y. Ishimi, H. Nagasawa, T. Matsumoto, J. Yanagisawa, S. Kato, Cell 113 (2003) 905–917.
[12] B. Lemon, C. Inouye, D.S. King, R. Tjian, Nature 414 (2001) 924–928.
[13] G.J. Narlikar, H.Y. Fan, R.E. Kingston, Cell 108 (2002) 475–487.
[14] W. Gu, S. Malik, M. Ito, C.X. Yuan, J.D. Fondell, X. Zhang, E. Martinez, J. Qin, R.G. Roeder, Mol. Cell 3 (1999) 97–108.
[15] C. Rachez, Z. Suldan, J. Ward, C.P. Chang, D. Burakov, H. Erdjument-Bromage, P. Tempst, L.P. Freedman, Genes Dev. 12 (1998) 1787–1800.
[16] T. Heinzel, R.M. Lavinsky, T.M. Mullen, M. Soderstrom, C.D. Laherty, J. Torchia, W.M. Yang, G. Brard, S.D. Ngo, J.R. Davie, E. Seto, R.N. Eisenman, D.W. Rose, C.K. Glass, M.G. Rosenfeld, Nature 387 (1997) 43–48.
[17] Y. Kamei, L. Xu, T. Heinzel, J. Torchia, R. Kurokawa, B. Gloss, S.C. Lin, R.A. Heyman, D.W. Rose, C.K. Glass, M.G. Rosenfeld, Cell 85 (1996) 403–414.
[18] S.A. Onate, S.Y. Tsai, M.J. Tsai, B.W. O'Malley, Science 270 (1995) 1354–1357.
[19] J. Yanagisawa, H. Kitagawa, M. Yanagida, O. Wada, S. Ogawa, M. Nakagomi, H. Oishi, Y. Yamamoto, H. Nagasawa, S.B. McMahon, M.D. Cole, L. Tora, N. Takahashi, S. Kato, Mol. Cell 9 (2002) 553–562.
[20] H. Hong, K. Kohli, A. Trivedi, D.L. Johnson, M.R. Stallcup, Proc. Natl. Acad. Sci. USA 93 (1996) 4948–4952.
[21] J.J. Voegel, M.J. Heine, C. Zechel, P. Chambon, H. Gronemeyer, EMBO J. 15 (1996) 3667–3675.
[22] S.L. Anzick, J. Kononen, R.L. Walker, D.O. Azorsa, M.M. Tanner, X.Y. Guan, G. Sauter, O.P. Kallioniemi, J.M. Trent, P.S. Meltzer, Science 277 (1997) 965–968.
[23] H. Chen, R.J. Lin, R.L. Schiltz, D. Chakravarti, A. Nash, L. Nagy, M.L. Privalsky, Y. Nakatani, R.M. Evans, Cell 90 (1997) 569–580.
[24] H. Li, P.J. Gomes, J.D. Chen, Proc. Natl. Acad. Sci. USA 94 (1997) 8479–8484.
[25] A. Takeshita, G.R. Cardona, N. Koibuchi, C.S. Suen, W.W. Chin, J. Biol. Chem. 272 (1997) 27629–27634.
[26] J. Torchia, D.W. Rose, J. Inostroza, Y. Kamei, S. Westin, C.K. Glass, M.G. Rosenfeld, Nature 387 (1997) 677–684.
[27] V.V. Ogryzko, R.L. Schiltz, V. Russanova, B.H. Howard, Y. Nakatani, Cell 87 (1996) 953–959.
[28] E. Metzger, M. Wissmann, N. Yin, J.M. Muller, R. Schneider, A.H. Peters, T. Gunther, R. Buettner, R. Schule, Nature 437 (2005) 436–439.
[29] Y. Sedkov, E. Cho, S. Petruk, L. Cherbas, S.T. Smith, R.S. Jones, P. Cherbas, E. Canaani, J.B. Jaynes, A. Mazo, Nature 426 (2003) 78–83.
[30] K. Takeyama, Y. Masuhiro, H. Fuse, H. Endoh, A. Murayama, S. Kitanaka, M. Suzawa, J. Yanagisawa, S. Kato, Mol. Cell. Biol. 19 (1999) 1049–1055.
[31] D.M. Heery, E. Kalkhoven, S. Hoare, M.G. Parker, Nature 387 (1997) 733–736.
[32] A.K. Shiau, D. Barstad, P.M. Loria, L. Cheng, P.J. Kushner, D.A. Agard, G.L. Greene, Cell 95 (1998) 927–937.
[33] A.K. Shiau, D. Barstad, J.T. Radek, M.J. Meyers, K.W. Nettles, B.S. Katzenellenbogen, J.A. Katzenellenbogen, D.A. Agard, G.L. Greene, Nat. Struct. Biol. 9 (2002) 359–364.
[34] T. Yoshizawa, Y. Handa, Y. Uematsu, S. Takeda, K. Sekine, Y. Yoshihara, T. Kawakami, K. Arioka, H. Sato, Y. Uchiyama, S. Masushige, A. Fukamizu, T. Matsumoto, S. Kato, Nat. Genet. 16 (1997) 391–396.
[35] T. Imai, K. Matsuda, T. Shimojima, T. Hashimoto, Y. Masuhiro, T. Kitamoto, A. Sugita, K. Suzuki, H. Matsumoto, S. Masushige, Y. Nogi, M. Muramatsu, H. Handa, S. Kato, Biochem. Biophys. Res. Commun. 233 (1997) 765–769.

[36] Y. Shang, X. Hu, J. DiRenzo, M.A. Lazar, M. Brown, Cell 103 (2000) 843–852.
[37] K.S. Chen, H.F. DeLuca, Biochim. Biophys. Acta 1263 (1995) 1–9.
[38] R. Fujiki, M.S. Kim, Y. Sasaki, K. Yoshimura, H. Kitagawa, S. Kato, EMBO J. 24 (2005) 3881–3894.
[39] V. Kumar, P. Chambon, Cell 55 (1988) 145–156.
[40] J.J. Voegel, M.J. Heine, M. Tini, V. Vivat, P. Chambon, H. Gronemeyer, EMBO J. 17 (1998) 507–519.
[41] C.X. Yuan, M. Ito, J.D. Fondell, Z.Y. Fu, R.G. Roeder, Proc. Natl. Acad. Sci. USA 95 (1998) 7939–7944.
[42] C. Rachez, B.D. Lemon, Z. Suldan, V. Bromleigh, M. Gamble, A.M. Naar, H. Erdjument-Bromage, P. Tempst, L.P. Freedman, Nature 398 (1999) 824–828.
[43] B. Belandia, R.L. Orford, H.C. Hurst, M.G. Parker, EMBO J. 21 (2002) 4094–4103.
[44] L.P. Freedman, Cell 97 (1999) 5–8.

nature medicine

Central control of bone remodeling by neuromedin U

Shingo Sato[1], Reiko Hanada[2], Ayako Kimura[1], Tomomi Abe[3], Takahiro Matsumoto[4,5], Makiko Iwasaki[1], Hiroyuki Inose[1], Takanori Ida[2], Michihiro Mieda[3], Yasuhiro Takeuchi[6], Seiji Fukumoto[7], Toshiro Fujita[7], Shigeaki Kato[4,5], Kenji Kangawa[8], Masayasu Kojima[2], Ken-ichi Shinomiya[1] & Shu Takeda[1]

Bone remodeling, the function affected in osteoporosis, the most common of bone diseases, comprises two phases: bone formation by matrix-producing osteoblasts[1] and bone resorption by osteoclasts[2]. The demonstration that the anorexigenic hormone leptin[3–5] inhibits bone formation through a hypothalamic relay[6,7] suggests that other molecules that affect energy metabolism in the hypothalamus could also modulate bone mass. Neuromedin U (NMU) is an anorexigenic neuropeptide that acts independently of leptin through poorly defined mechanisms[8,9]. Here we show that *Nmu*-deficient (*Nmu*$^{-/-}$) mice have high bone mass owing to an increase in bone formation; this is more prominent in male mice than female mice. Physiological and cell-based assays indicate that NMU acts in the central nervous system, rather than directly on bone cells, to regulate bone remodeling. Notably, leptin- or sympathetic nervous system–mediated inhibition of bone formation[6,7] was abolished in *Nmu*$^{-/-}$ mice, which show an altered bone expression of molecular clock genes (mediators of the inhibition of bone formation by leptin). Moreover, treatment of wild-type mice with a natural agonist for the NMU receptor decreased bone mass. Collectively, these results suggest that NMU may be the first central mediator of leptin-dependent regulation of bone mass identified to date. Given the existence of inhibitors and activators of NMU action[10], our results may influence the treatment of diseases involving low bone mass, such as osteoporosis.

Bone mass is maintained at a constant level between puberty and menopause by a succession of bone-resorption and bone-formation phases[11,12]. The discovery that neuronal control of bone remodeling is mediated by leptin[6] shed light on a new regulatory mechanism of bone remodeling and also suggested that bone mass may be regulated by a variety of neuropeptides[13]. In line with this observation, cannabinoids and pituitary hormones have been shown to be intimately involved in bone remodeling[14,15]. Leptin inhibits bone formation by binding to its receptors located in hypothalamus and thereby activating the sympathetic nervous system (SNS), which requires the adrenergic β2 receptors (Adrb2) expressed in osteoblasts[7,16]. Downstream of Adrb2, leptin signaling activates molecular clock genes that regulate osteoblast proliferation and hence bone formation[17]. In addition, leptin regulates bone resorption through two distinct pathways[16].

NMU is a small peptide produced by nerve cells in the submucosal and myenteric plexuses in the small intestine, and also by structures in the brain, including the dorsomedial nucleus of the hypothalamus[9]. It is generally assumed that NMU acts as a neuropeptide to regulate various aspects of physiology, including appetite, stress response and SNS activation[9]. Indeed, NMU-deficient (*Nmu*$^{-/-}$) mice develop obesity due to increased food intake and reduced locomotor activity that is believed, at least in part, to be leptin independent[8]. In addition, expression of NMU is diminished in leptin-deficient (*Lep*^{ob}) mice[18], but can be induced in these mice by leptin treatment[19]. In search of additional neuropeptides that regulate bone remodeling, we analyzed *Nmu*$^{-/-}$ mice.

When assessed at 3 and 6 months of age, both male and female *Nmu*$^{-/-}$ mice showed a high bone mass phenotype as compared to the wild type (WT), with male mice more severely affected than female mice (**Fig. 1a** and data not shown). The presence of a uniform increase in bone mineral density (BMD) along the femurs of *Nmu*$^{-/-}$ mice suggested that both trabecular and cortical bone were equally affected (**Supplementary Fig. 1** online). Microcomputed tomography analysis confirmed this observation (**Fig. 1b,c**). To determine whether this phenotype was secondary to the obesity of the *Nmu*$^{-/-}$ mice, we restricted their food intake for 1 month starting at 2 months of age. This manipulation normalized the body weight and serum insulin level of the *Nmu*$^{-/-}$ mice but did not affect their high bone mass phenotype (**Fig. 1d** and data not shown). Of note, when *Nmu*$^{-/-}$ mice were backcrossed to the C57BL/6J genetic background, their body weight became similar to that of their WT littermates; however, their BMD remained high (data not shown). These results suggest that NMU regulates bone mass independently of its regulation of energy metabolism, just as leptin does[7]. To better characterize the cellular nature of the bone phenotype in the *Nmu*$^{-/-}$ mice, we

[1]Department of Orthopaedic Surgery, Graduate School, 21st Century Center of Excellence Program, Tokyo Medical and Dental University, 1-5-45 Yushima, Bunkyo-ku, Tokyo 113-8519, Japan. [2]Division of Molecular Genetics, Institute of Life Science, Kurume University, 1-1 Hyakunen-kohen, Kurume, Fukuoka 839-0842, Japan. [3]Department of Molecular Neuroscience, Tokyo Medical and Dental University 1-5-45 Yushima, Bunkyo-ku, Tokyo 113-8519, Japan. [4]Institute of Molecular and Cellular Biosciences, University of Tokyo, 1-1-1 Yayoi, Bunkyo-ku, Tokyo 113-0032, Japan. [5]Exploratory Research for Advanced Technology, Japan Science and Technology Agency, 4-1-8 Honcho, Kawaguchi, Saitama 332-0012, Japan. [6]Toranomon Hospital Endocrine Center, 2-2-2 Toranomon, Minato-ku, Tokyo 105-8470, Japan. [7]Division of Nephrology and Endocrinology, Department of Internal Medicine, University of Tokyo Hospital, 7-3-1 Hongo, Bunkyo-ku, Tokyo 113-8655, Japan. [8]Department of Biochemistry, National Cardiovascular Center Research Institute, 5-7-1 Fujishiro-dai, Suita-shi, Osaka 565-8565, Japan. Correspondence should be addressed to S.T. (shu-tky@umin.ac.jp).

Received 4 June; accepted 8 August; published online 16 September 2007; doi:10.1038/nm1640

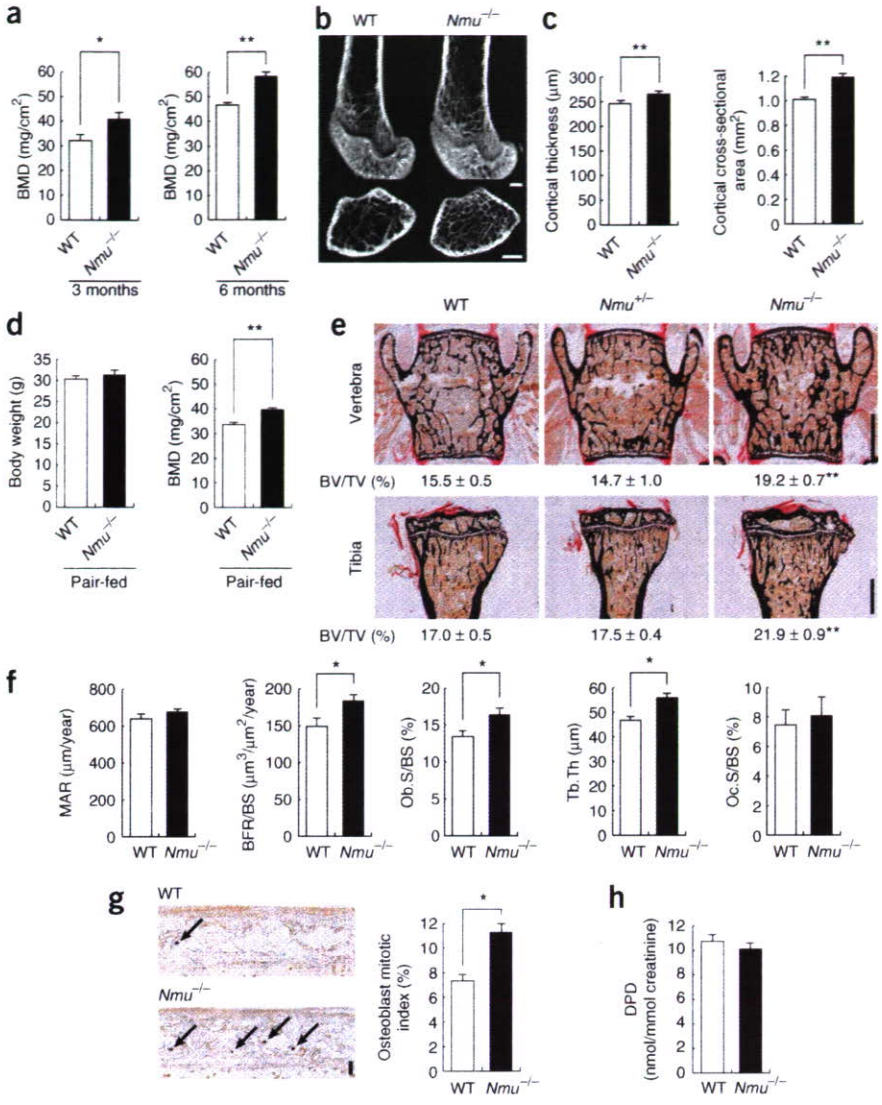

Figure 1 High bone mass in *Nmu*$^{-/-}$ mice due to increased bone formation. (**a**) Bone mineral density (BMD) of the femurs of 3 (left)- and 6 (right)-month-old male wild-type (WT) and *Nmu*$^{-/-}$ mice. (**b**) Micro-computed tomography (μCT) analysis of the distal femurs of male mice at 3 months. Scale bars, 500 μm. (**c**) Cortical thickness and cross-sectional area of the femurs of 3-month-old male mice. (**d**) Body weight and BMD of 3-month-old male mice with restricted food intake. (**e**) Histological analysis of the vertebrae and tibiae of 3-month-old male WT, *Nmu*$^{+/-}$ and *Nmu*$^{-/-}$ mice. Bone volume per tissue volume (BV/TV). Scale bars, 1 mm. (**f**) Histomorphometric analysis of the vertebrae of 3-month-old male mice. Mineral apposition rate (MAR), bone formation rate over bone surface area (BFR/BS), osteoblast surface area over bone surface area (Ob.S/BS), trabecular thickness (Tb. Th) and osteoclast surface area over bone surface area (Oc.S/BS). (**g**) Increased osteoblast proliferation in newborn *Nmu*$^{-/-}$ mice. Immunolocalization of BrdU incorporation (arrows) in the calvariae of WT and *Nmu*$^{-/-}$ mice (left). Osteoblast mitotic index (right). Scale bar, 20 μm. (**h**) Urinary elimination of deoxypyridinoline (DPD) in WT and *Nmu*$^{-/-}$ mice. **, $P < 0.01$; *, $P < 0.05$.

performed histological and histomorphometric analyses of vertebrae and tibiae in both male and female animals (**Fig. 1e** and **Supplementary Fig. 1**). At 3 and 6 months of age, *Nmu*$^{-/-}$ mice showed greater bone volume in both vertebrae and tibiae than did WT littermates, with male mice having a more pronounced phenotype (**Fig. 1e** and **Supplementary Fig. 1**). At the present time we do not have a clear explanation of the difference in phenotype severity between male and female mice. Bone formation rates (WT mice, 146.9 ± 12.3, *Nmu*$^{-/-}$ mice, 183.7 ± 10.3, $P < 0.05$) and osteoblast numbers were both significantly greater in the vertebrae and tibiae of *Nmu*$^{-/-}$ mice (**Fig. 1f** and **Supplementary Fig. 1**). The higher osteoblast numbers in the presence of a normal mineral apposition rate (**Fig. 1f** and **Supplementary Fig. 1**), which reflects the function of individual osteoblasts[20], suggested that osteoblast proliferation may be increased in *Nmu*$^{-/-}$ mice. Indeed, 5-bromo-2-deoxyuridine (BrdU)-positive proliferative osteoblast counts were significantly increased in *Nmu*$^{-/-}$ mice *in vivo* (**Fig. 1g**), demonstrating that NMU affects osteoblast proliferation. In contrast, *Nmu*$^{-/-}$ and WT mice showed comparable osteoclast numbers and osteoclast surface areas (**Fig. 1f** and **Supplementary Fig. 1**), suggesting that NMU does not affect bone resorption. This observation was further supported by the normal level of urinary elimination of deoxypyridinoline in *Nmu*$^{-/-}$ mice (**Fig. 1h**).

Taken together, these results demonstrate that NMU deficiency results in an isolated increase in bone formation leading to high bone mass. *Nmu*-heterozygote mice did not have an overt bone abnormality at any age analyzed (**Fig. 1e**).

Two cognate G protein–coupled receptors have been reported to be NMU receptors: NMUR1, which is expressed in various tissues, including the small intestine and lung (data not shown), and NMUR2, which is predominantly expressed in the hypothalamus and the small intestine (**Fig. 2a**)[18]. Both receptors and NMU itself were barely detectable in bone (**Fig. 2a**). To further exclude the possibility of a direct action of NMU on osteoblasts, we treated mouse primary osteoblasts with varying concentrations of NMU. Alkaline phosphatase activity, mineralization and expression of osteoblastic genes were all unaffected by this treatment (**Fig. 2b,c**). In addition, there were no differences between WT mice and *Nmu*$^{-/-}$ mice in the expression of osteoblastic genes *in vivo* (**Fig. 2d**). Moreover, both WT and *Nmu*$^{-/-}$ osteoblasts proliferated normally *in vitro* in response to NMU treatment (**Fig. 2e**), though *Nmu*$^{-/-}$ osteoblasts proliferated more than WT osteoblasts *in vivo* (**Fig. 1g**). Osteoclastic differentiation from bone marrow macrophages was unchanged by NMU treatment (**Fig. 2f**), as expected from the absence of a bone resorption defect *in vivo* (**Fig. 1f,h**). Taken together, these results strongly suggest that NMU's effect on bone may not come from its direct action on osteoblasts, but rather through another relay.

Because the anorexigenic effect of NMU requires a hypothalamic relay[8,19] and because hypothalamic neurons have been shown to regulate bone mass, we tested whether NMU's regulation of bone formation could involve a central relay. Continuous intracerebroventricular (i.c.v.) infusion of NMU into *Nmu*$^{-/-}$ mice decreased their fat mass and fat pad weight significantly, although body weight was not

affected (**Fig. 2g** and **Supplementary Fig. 2** online). In addition, NMU i.c.v. infusion eliminated the high bone mass phenotype in *Nmu*$^{-/-}$ mice (**Fig. 2g** and **Supplementary Fig. 2**), suggesting that NMU inhibits bone formation through the central nervous system.

The central nature of bone remodeling regulation by NMU, along with the notion that the anorexigenic effect of NMU may be independent of leptin[8], prompted us to examine whether leptin could be involved in the regulation of bone formation by NMU. To address this question, we performed i.c.v. infusion of NMU or leptin in *Lep*^{ob} mice. NMU decreased fat pad weight significantly, albeit to a milder extent than that achieved by leptin (**Fig. 3a** and **Supplementary Fig. 3** online). Body weight was not significantly changed by the NMU infusion, indicating that this treatment had only a mild effect on energy metabolism (data not shown). In contrast, NMU decreased bone mass in *Lep*^{ob} mice as efficiently as leptin did (**Fig. 3a**). These results indicate that NMU inhibits bone formation in a leptin-independent manner. Next, we asked whether leptin could correct the high bone mass phenotype of *Nmu*$^{-/-}$ mice. Leptin i.c.v. infusion decreased bone volume and bone formation in WT mice, as previously reported (**Fig. 3b** and **Supplementary Fig. 3**)[6]. However, the leptin paradoxically increased bone volume and osteoblast number in *Nmu*$^{-/-}$ mice (**Fig. 3b,c** and **Supplementary Fig. 3**). The fact that leptin decreased fat mass and fat pad weight in *Nmu*$^{-/-}$ mice and increased urinary elimination of normetanephrine, a metabolite of noradrenaline[17], verified that the administration of leptin was properly performed (**Fig. 3b,d** and **Supplementary Fig. 3**). Therefore, taken together, these results suggest that NMU acts downstream of leptin to regulate bone formation.

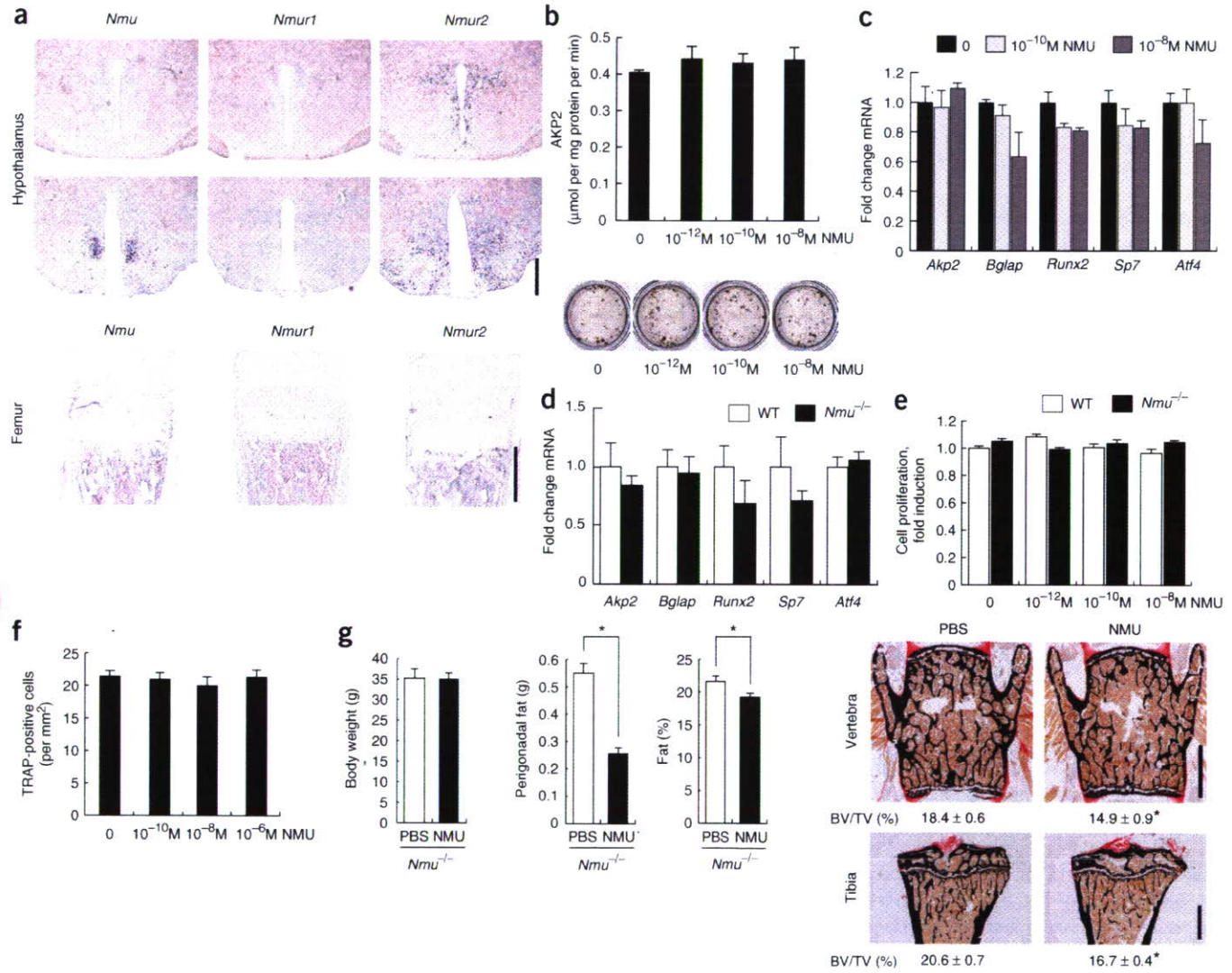

Figure 2 Absence of NMU's direct effect on osteoblasts; decrease in bone mass by NMU i.c.v. infusion. (**a**) Expression of *Nmu*, *Nmur1* and *Nmur2* in the hypothalamus at the atlas-levels of 38 (top) and 43 (bottom) and in the femur as shown by *in situ* hybridization. Note the expression of *Nmu* in the dorsomedial nucleus of the hypothalamus (DMH) (bottom) and *Nmur2* in paraventricular nucleus (top), arcuate nucleus and DMH (bottom). Scale bars, 500 μm. (**b–d**) Effect of NMU on osteoblast differentiation. (**b,c**) WT osteoblasts treated with NMU. (**b**) Alkaline phosphatase (AKP2) activity (top), mineralized nodule formation (bottom). (**c**) Expression of osteoblastic genes (*Akp2*, *Bglap*, *Runx2*, *Sp7* and *Atf4*), depicted as fold change over WT expression. (**d**) Expression of osteoblastic genes in WT and *Nmu*$^{-/-}$ femurs. (**e**) Effect of NMU on osteoblast proliferation. WT or *Nmu*$^{-/-}$ osteoblasts treated with NMU. (**f**) Effect of NMU on osteoclast differentiation. Bone marrow–derived osteoclasts treated with NMU. (**g**) Effect of NMU i.c.v. infusion on body weight, fat pad weight (perigonadal fat) and fat mass (left). Histological analysis of the vertebrae (top right) and tibiae (bottom right). Male mice at 3 months of age were used. Scale bars, 1 mm. *, $P < 0.05$.

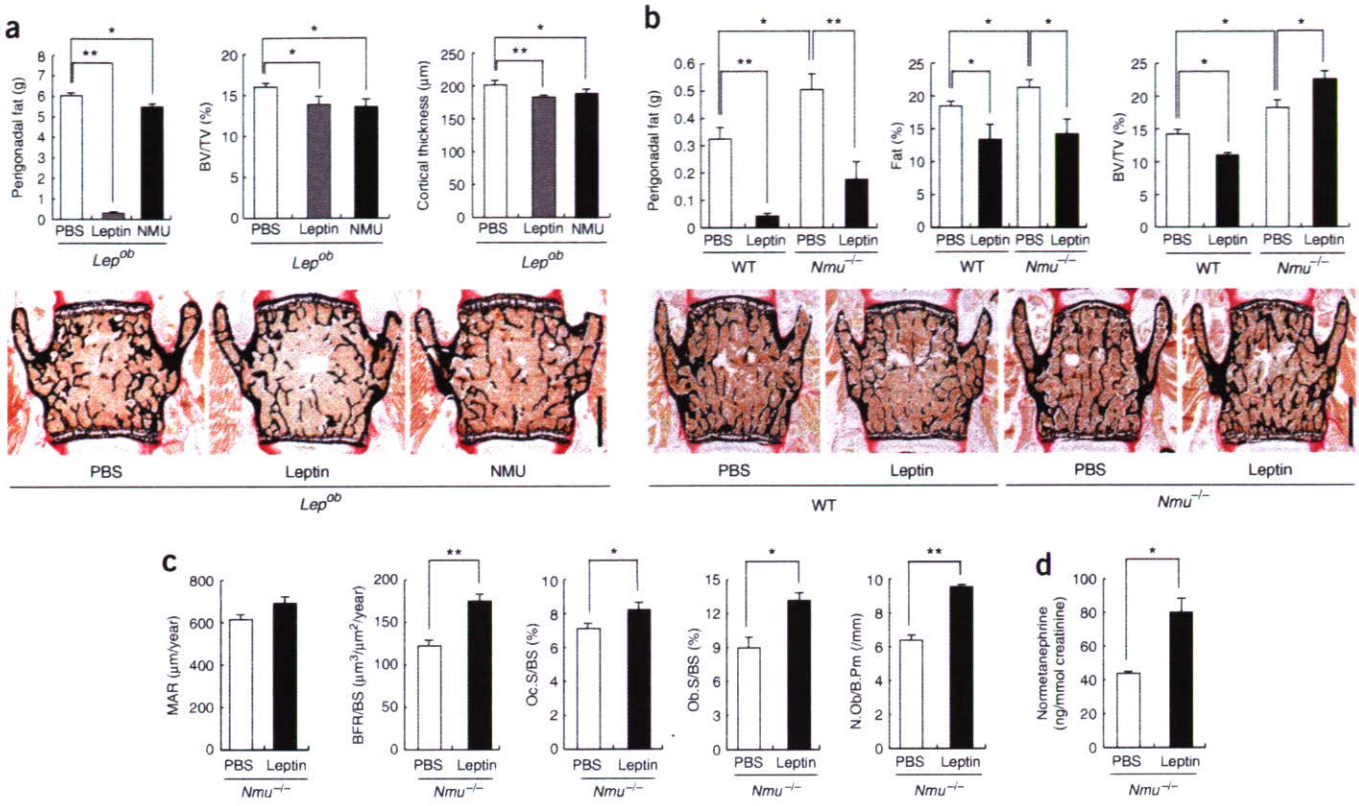

Figure 3 Leptin does not eliminate high bone mass in *Nmu*$^{-/-}$ mice. (**a**) Effect of NMU or leptin i.c.v. infusion in *Lep*^{ob} mice (3-month-old males). Fat pad weight and bone mass were determined by histology and cortical thickness by μCT analysis. (**b–d**) Effect of leptin i.c.v. infusion on *Nmu*$^{-/-}$ mice (3-month-old males). (**b**) Fat pad weight, fat mass and bone mass shown by histology. (**c**) Histomorphometric analysis. N. Ob/B.Pm indicates the number of osteoblasts per bone perimeter. (**d**) Urinary elimination of normetanephrine. Scale bars, 1 mm. **, $P < 0.01$; *, $P < 0.05$.

The SNS is a major mediator of leptin's antiosteogenic action[7]. NMUR2 is expressed in paraventricular nuclei, whose neurons directly project to the sympathetic preganglionic neurons, and NMU stimulates sympathetic outflow[9,21]. These observations, along with the fact that *Nmu*$^{-/-}$ mice have osteoblastic defects similar to the one observed in *Adrb2*-deficient mice[16], prompted us to explore whether NMU and sympathetic tone are in the same pathway regulating bone formation. Indeed, *Nmu/Adrb2* double heterozygote mice had higher bone mass than *Adrb2* single heterozygote mice (**Fig. 4a**), although *Nmu* single heterozygote mice had normal bone mass (**Fig. 1e** and **Supplementary Fig. 1**). Given that *Nmu* expression in the hypothalamus was reduced in *Nmu* single heterozygote mice (data not shown), compound heterozygosity of *Nmu* and *Adrb2* may have resulted in higher bone mass. Furthermore, this result suggests that these two pathways share a common molecule. Of note, *Nmu*$^{-/-}$ mice had a higher degree of urinary elimination of normetanephrine than WT littermates (**Fig. 4b**), which would decrease bone mass, yet they had high bone mass. This suggests that their high bone mass phenotype is not caused by decreased SNS activity, but is instead the result of resistance to the antiosteogenic activity of the SNS. This is in agreement with the observation that i.c.v. infusion of leptin, a potent stimulator of SNS activity, did not decrease bone mass in *Nmu*$^{-/-}$ mice (**Fig. 3b** and **Supplementary Fig. 3**). Furthermore, injection of isoproterenol, a sympathomimetic, reduced bone mass in WT mice[7] but not in *Nmu*$^{-/-}$ mice (**Fig. 4c** and **Supplementary Fig. 4** online). Thus, *Nmu*$^{-/-}$ mice are resistant to the antiosteogenic effects of both leptin and the SNS.

We present six experimental arguments to strongly suggest that the failure of leptin or isoproterenol to decrease bone mass in *Nmu*$^{-/-}$ mice is not due to leptin-SNS signaling defects. First, leptin infusion decreased fat pad weight equally well in WT and in *Nmu*$^{-/-}$ mice and could increase normetanephrine abundance in *Nmu*$^{-/-}$ mice (**Fig. 3b,d** and **Supplementary Fig. 3**). Second, the expression of *Adrb2* was not different in WT and *Nmu*$^{-/-}$ bones (**Fig. 4d**). Third, treatment with NMU did not affect *Adrb2* expression in osteoblasts (**Supplementary Fig. 5** online). Fourth, isoproterenol induced expression of *Tnfsf11* (encoding tumor necrosis factor superfamily, member 11) and decreased expression of *Tnfrsf11b* (encoding tumor necrosis factor superfamily, member 11b, also known as osteoprotegerin), *Runx2* (encoding runt-related transcription factor-2) and *Col1a1* (encoding collagen type I), molecular markers for the effect of SNS activation on osteoblasts, in both WT and *Nmu*$^{-/-}$ osteoblasts (**Fig. 4d**). Fifth, isoproterenol induced cAMP production equally well in WT and *Nmu*$^{-/-}$ osteoblasts (**Fig. 4e**). Sixth, and most notably, leptin increased bone resorption to a similar extent in WT and *Nmu*$^{-/-}$ mice (**Fig. 3c** and **Supplementary Fig. 3**).

The fact that the leptin-SNS pathway is intact in *Nmu*$^{-/-}$ mice, together with the paradoxical increase in osteoblast number induced by leptin i.c.v. infusion in *Nmu*$^{-/-}$ mice (**Fig. 3c**), suggests that NMU affects only the negative regulator of bone remodeling by leptin, that is, the molecular clock. Indeed, the expression of *Per1* and *Per2* (encoding period homolog-1 and -2, respectively) was downregulated in *Nmu*$^{-/-}$ bones as compared to WT bones (**Fig. 4f** and **Supplementary Fig. 6** online). Thus, NMU, acting through the central nervous system, affects the molecular clock in bone.

Because bone resorption in *Nmu*$^{-/-}$ mice was comparable to that in the wild type, despite the high SNS activity in these mice, we also

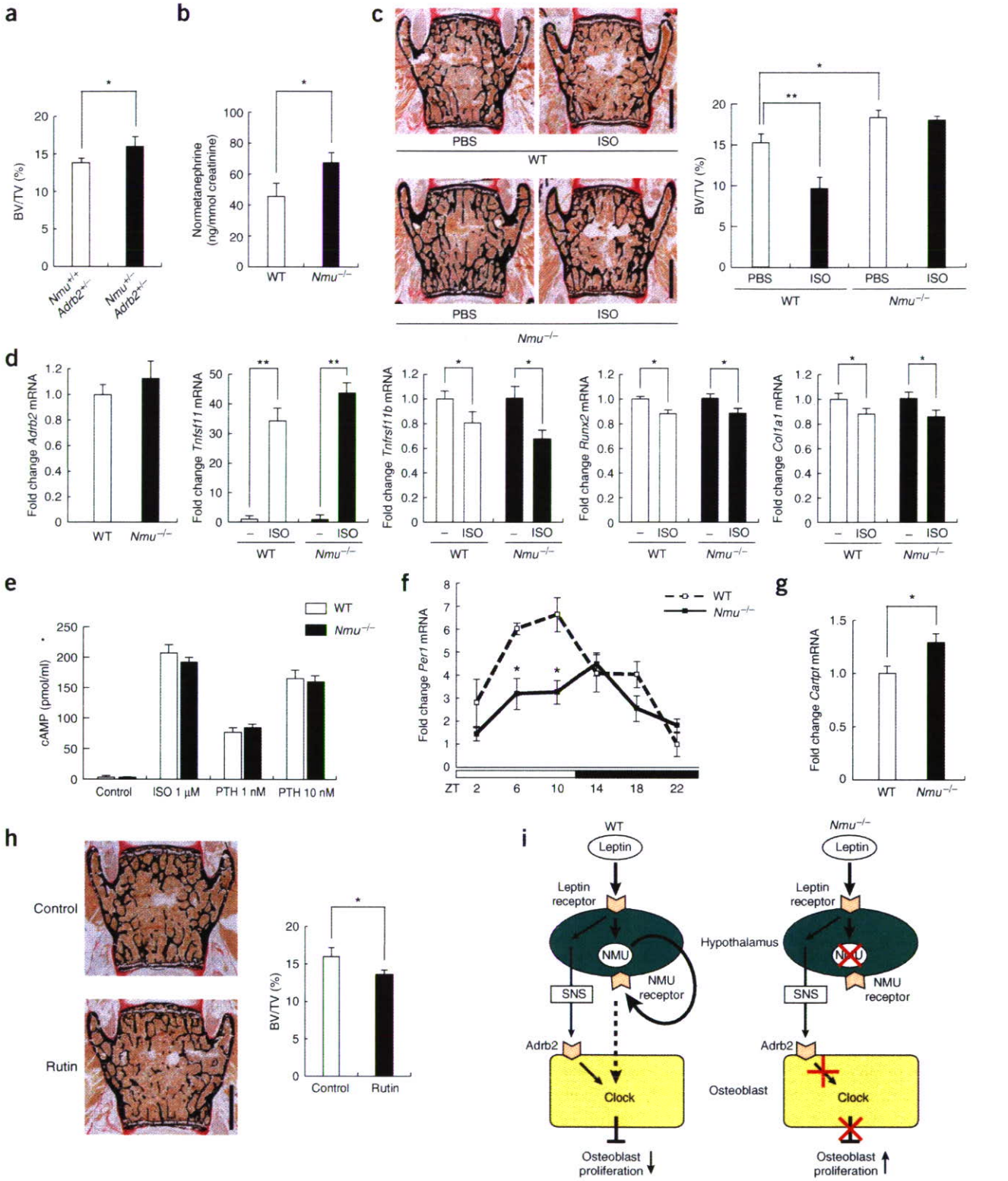

Figure 4 Sympathetic activation does not rescue high bone mass in *Nmu*$^{-/-}$ mice. (**a**) Bone mass in *Adrb2*$^{+/-}$/*Nmu*$^{+/-}$and *Adrb2*$^{+/-}$/*Nmu*$^{+/+}$ mice as determined by histology (3-month-old males). (**b**) Increased urinary elimination of normetanephrine in *Nmu*$^{-/-}$ mice. (**c**) Effect of sympathetic activation by isoproterenol (ISO) injection in *Nmu*$^{-/-}$ mice (3-month-old males). Shown is the bone mass of vertebrae as determined by histology. (**d**) Expression of *Adrb2* in the femurs of WT and *Nmu*$^{-/-}$ mice (left). Gene expression changes induced by isoproterenol (ISO) treatment of WT and Nmu$^{-/-}$ osteoblasts (four rightmost graphs). (**e**) cAMP concentration in the culture medium of WT and *Nmu*$^{-/-}$ osteoblasts after ISO treatment. Parathyroid hormone (PTH) was used as a control. (**f**) Expression of *Per1* in the femurs of WT and *Nmu*$^{-/-}$ mice. Zeitberger time (ZT) is indicated on the *x*-axis. (**g**) Expression of *Cartpt* in the hypothalamus of WT and *Nmu*$^{-/-}$ mice. (**h**) Rutin decreases bone mass in WT mice as determined by histological analysis of vertebrae (left) and quantitative histomorphometric analysis (right) (3-month-old males). Scale bar, 1 mm. **, $P < 0.01$; *, $P < 0.05$. (**i**) Model of leptin, sympathetic nervous system (SNS) and NMU signaling for the regulation of bone formation in WT mice (left) and *Nmu*$^{-/-}$ mice (right).

tested whether the expression of *Cartpt* (encoding cocaine- and amphetamine-regulated transcript propeptide), a central mediator of leptin's action on bone resorption[16], was altered in these mice. Indeed, *Cartpt* expression was increased in $Nmu^{-/-}$ mice as compared to WT littermates (**Fig. 4g** and **Supplementary Fig. 7** online). These results suggest that the protective activity of Cart on bone resorption compensates for the bone-resorbing activity induced by the SNS in $Nmu^{-/-}$ mice. The effect of other leptin-regulated neuropeptides, such as NPY (neuropeptide Y), AgRP (agouti-related protein) and α-MSH (α-melanotropin), will be limited, because the expression of *Npy* and *Agrp* was unchanged in $Nmu^{-/-}$ mice[8] and melanocortin 4 receptor, a major receptor for α-MSH, has been shown to have little effect on bone remodeling by itself[22].

Lastly, we treated WT mice with rutin, a natural NMUR2 agonist found in daily foods such as buckwheat[23]. Consistent with the high bone mass phenotype of the $Nmu^{-/-}$ mice, rutin decreased bone mass significantly in WT mice (**Fig. 4h**). This result, together with the predominant expression of *Nmur2* in the hypothalamus (**Fig. 2a**), suggests that NMU regulates bone remodeling through NMUR2.

Collectively, these results suggest that NMU, through a central relay and via an unidentified pathway, acts as a modulator of leptin-SNS-Adrb2 regulation of bone formation (**Fig. 4i**). However, one concern still remains: because leptin affects several pathways originating in the hypothalamus and elsewhere in the brain, i.c.v. infusion of leptin may have resulted in an uncoordinated change in leptin-regulated bone remodeling that does not reflect a physiological role of leptin. To rigorously address that question, an analysis of a mouse model in which a specific nucleus of the hypothalamus is activated by leptin will be necessary. From a therapeutic point of view, given the lack of an obesity phenotype in *Nmur2*-deficient mice[24], an NMU antagonist may be a candidate for the treatment of bone-loss disorders without inducing unwanted body weight gain.

METHODS

Animals. $Nmu^{-/-}$ and $Adrb2^{-/-}$ mice were previously described[8,16]. We purchased C57BL/6J mice and C57BL/6J Lep^{ob} from the Jackson Laboratory. We maintained all of the mice under a 12 hr light-dark cycle with *ad libitum* access to regular food and water, unless specified. For pair-fed experiments, we caged $Nmu^{-/-}$and WT mice individually for 12 weeks as described[8]. In brief, $Nmu^{-/-}$ mice were given access to water *ad libitum* and fed the amount of chow eaten on the previous day by a WT littermate. We determined mouse genotypes by PCR as previously described[8,16]. We injected isoproterenol (10 mg/kg, Sigma) intraperitoneally (i.p.) once daily for 4 weeks. Rutin (Sigma) was administered orally 300 mg per kg body weight per day for 4 weeks. All animal experiments were performed with the approval of the Animal Study Committee of Tokyo Medical and Dental University and conformed to relevant guidelines and laws.

Dual X-ray absorptiometry and microcomputed tomography analysis. We measured bone mineral density (BMD) of the femurs and fat pad composition by DCS–600 (Aloka). We obtained two-dimensional images of the distal femurs by microcomputed tomography (μCT, Comscan). We measured cortical thickness and cross-sectional area at the center of the femur. We examined at least eight mice for each group.

Histological and histomorphometric analysis. We injected calcein (25 mg/kg, Sigma) i.p. 5 and 2 d before sacrifice. We stained undecalcified sections of the third and fourth lumbar vertebrae and tibiae with von Kossa staining. We performed static and dynamic histomorphometric analyses using the Osteomeasure Analysis System (Osteometrics). We analyzed 8–10 mice for each group.

***In situ* hybridization analysis.** We performed *in situ* hybridization analysis according to the established protocol[25]. Antisense cRNA probe for *Cartpt* was previously described[26]. We used fragments of cDNA for *Nmu* (105 base pairs upstream to 647 base pairs downstream of the initiation codon), *Nmur1* (13–1242 base pairs downstream of the initiation codon) and *Nmur2* (16–1252 base pairs downstream of the initiation codon) to generate antisense probes. We stained sections hybridized with ^{35}S-labeled probes with Hoechst 33528 and quantitatively analyzed the expression of *Cartpt* with a phosphorimager (Bass–2500, Fuji). The atlas-level of designations corresponds to those described previously[27]. We analyzed six mice for each group.

Measurement of deoxypyridinoline cross-links and normetanephrine. We measured urinary deoxypyridinoline cross-links (DPD) and normetanephrine with the METRA DPD-EIA kit (Quidel) and the Normetanephrine-ELISA kit (ALPCO), respectively, according to the manufacturer's instructions. We used creatinine values to standardize between samples (Creatinine Assay Kit, Cayman). We examined eight samples for each group.

Cell culture. *In vitro* primary osteoblast cultures were established as previously described[6]. Briefly, we cultured primary osteoblasts from calvariae of 4-d-old mice in α-MEM (Sigma) containing ascorbic acid (0.1 mg/ml, Sigma). We added NMU to the medium twice daily. After 14 d, we measured alkaline phosphatase activity with the ALP kit (Wako). For the mineralization assay, we supplemented the medium with β-glycerophosphate (5 mM, Sigma). We assessed mineralized nodule formation by von Kossa staining. We performed the cell proliferation and cAMP assays with the Cell Proliferation Assay (Promega) and cAMP EIA kit (Cayman Chemical), respectively. *In vitro* osteoclast differentiation has been described previously[16]. Briefly, bone marrow cells of 2-month-old mice were cultured in the presence of human macrophage colony-stimulating factor (10 ng/ml, R&D Systems) for 2 d and then differentiated into osteoclasts with human RANKL (50 ng/ml, Peprotech) and human macrophage colony-stimulating factor (10 ng/ml) for 3 d. We counted tartrate-resistant acid phosphatase (TRAP)-positive multinucleated cells (more than 3 nuclei). We performed all the cell cultures in triplicate or quadruplicate wells and repeated more than 3 times.

BrdU immunohistochemistry. For BrdU labeling, we injected 100 μg BrdU i.p. into 3-d-old mice 1 h before sacrifice. We embedded calvariae in paraffin and cut coronally. We detected BrdU-incorporated osteoblasts with the BrdU Immunohistochemistry Kit (Exalpha Biologicals). We calculated the number of BrdU-positive osteoblasts over the total number of osteoblasts (osteoblast mitotic index) at three different locations (+3.0, 3.5 and 4.0 AP (0 point: bregma)) per mouse. We analyzed six mice per group.

Intracerebroventricular infusion. Intracerebroventricular infusion was performed as previously described[6]. Briefly, we exposed the calvaria of an anesthetized mouse, implanted a 28-gauge cannula (Plastics ONE) into the third ventricle and then connected the cannula to an osmotic pump (Durect) placed in the dorsal subcutaneous space of the mouse. We infused rat Neuromedin U-23 (Peptide Institute) or human leptin (Sigma) at 0.125 nmol/hr or 8 ng/hr, respectively, for 28 d.

Quantitative RT–PCR analysis. After flushing mouse bone marrow out of the bone with PBS, we extracted bone RNA with Trizol (Invitrogen) and performed reverse transcription for cDNA synthesis. We performed quantitative analysis of gene expression with the Mx3000P real-time PCR system (Stratagene). Primer sequences are available upon request. We used GAPDH expression as an internal control.

Statistical analysis. All data are represented as mean ± s.d. ($n = 8$ or more). We performed statistical analysis by Student's *t*-test. Values were considered statistically significant at $P < 0.05$. Results are representative of more than four individual experiments.

Note: Supplementary information is available on the Nature Medicine website.

ACKNOWLEDGMENTS

We thank G. Karsenty, M. Patel and P. Ducy for critical review of the manuscript and for helpful discussions; K. Nakao, M. Noda, T. Matsumoto and S. Ito for insightful suggestions; P. Barrett (Rowett Research Institute, UK) for providing a plasmid for the *Cartpt* probe; and J. Chen, M. Starbuck, S. Sunamura, H. Murayama, H. Yamato, and M. Kajiwara for technical assistance. This work was supported by grant-in-aid for scientific research from the Japan Society for

the Promotion of Science, a grant for the 21st Century Center of Excellence program from the Ministry of Education, Culture, Sports, Science, and Technology of Japan, Ono Medical Research Foundation, Yamanouchi Foundation for Research on Metabolic Disorders, Kanae Foundation for the Promotion of the Medical Science and the Program for Promotion of Fundamental Studies in Health Sciences of the National Institute of Biomedical Innovation of Japan.

AUTHOR CONTRIBUTIONS

S. Sato conducted most of the experiments. K. Kangawa and M. Kojima generated *Nmu*$^{-/-}$ mice. R. Hanada and T. Ida conducted *in vitro* experiments. S. Fukumoto, Y. Takeuchi and T. Fujita contributed by conducting dual X-ray absorptiometry analyses and providing suggestions on the project. M. Iwasaki prepared the constructs. A. Kimura performed i.c.v. infusion experiments. H. Inose conducted μCT analyses. T. Matsumoto and S. Kato conducted histological analyses for brain tissue. T. Abe and M. Mieda performed *in situ* hybridization analysis. S. Takeda and K. Shinomiya designed the project. S. Takeda supervised the project and wrote most of the manuscript.

Published online at http://www.nature.com/naturemedicine
Reprints and permissions information is available online at http://npg.nature.com/reprintsandpermissions

1. Rodan, G.A. & Martin, T.J. Therapeutic approaches to bone diseases. *Science* **289**, 1508–1514 (2000).
2. Teitelbaum, S.L. & Ross, F.P. Genetic regulation of osteoclast development and function. *Nat. Rev. Genet.* **4**, 638–649 (2003).
3. Saper, C.B., Chou, T.C. & Elmquist, J.K. The need to feed: homeostatic and hedonic control of eating. *Neuron* **36**, 199–211 (2002).
4. Ahima, R.S. & Flier, J.S. Leptin. *Annu. Rev. Physiol.* **62**, 413–437 (2000).
5. Spiegelman, B.M. & Flier, J.S. Obesity and the regulation of energy balance. *Cell* **104**, 531–543 (2001).
6. Ducy, P. *et al.* Leptin inhibits bone formation through a hypothalamic relay: a central control of bone mass. *Cell* **100**, 197–207 (2000).
7. Takeda, S. *et al.* Leptin regulates bone formation via the sympathetic nervous system. *Cell* **111**, 305–317 (2002).
8. Hanada, R. *et al.* Neuromedin U has a novel anorexigenic effect independent of the leptin signaling pathway. *Nat. Med.* **10**, 1067–1073 (2004).
9. Brighton, P.J., Szekeres, P.G. & Willars, G.B. Neuromedin U and its receptors: structure, function, and physiological roles. *Pharmacol. Rev.* **56**, 231–248 (2004).
10. Fang, L., Zhang, M., Li, C., Dong, S. & Hu, Y. Chemical genetic analysis reveals the effects of NMU2R on the expression of peptide hormones. *Neurosci. Lett.* **404**, 148–153 (2006).
11. Riggs, B.L., Khosla, S. & Melton, L.J. 3rd. A unitary model for involutional osteoporosis: estrogen deficiency causes both type I and type II osteoporosis in postmenopausal women and contributes to bone loss in aging men. *J. Bone Miner. Res.* **13**, 763–773 (1998).
12. Karsenty, G. & Wagner, E.F. Reaching a genetic and molecular understanding of skeletal development. *Dev. Cell* **2**, 389–406 (2002).
13. Harada, S. & Rodan, G.A. Control of osteoblast function and regulation of bone mass. *Nature* **423**, 349–355 (2003).
14. Idris, A.I. *et al.* Regulation of bone mass, bone loss and osteoclast activity by cannabinoid receptors. *Nat. Med.* **11**, 774–779 (2005).
15. Abe, E. *et al.* TSH is a negative regulator of skeletal remodeling. *Cell* **115**, 151–162 (2003).
16. Elefteriou, F. *et al.* Leptin regulation of bone resorption by the sympathetic nervous system and CART. *Nature* **434**, 514–520 (2005).
17. Fu, L., Patel, M.S., Bradley, A., Wagner, E.F. & Karsenty, G. The molecular clock mediates leptin-regulated bone formation. *Cell* **122**, 803–815 (2005).
18. Howard, A.D. *et al.* Identification of receptors for neuromedin U and its role in feeding. *Nature* **406**, 70–74 (2000).
19. Wren, A.M. *et al.* Hypothalamic actions of neuromedin U. *Endocrinology* **143**, 4227–4234 (2002).
20. Parfitt, A.M. The physiological and clinical significance of bone histomorphometric data. in *Bone Histomorphometry* (ed. Recker, R.R.) 143–223 (CRC Press, Boca Raton, FL, 1983).
21. Chu, C. *et al.* Cardiovascular actions of central neuromedin U in conscious rats. *Regul. Pept.* **105**, 29–34 (2002).
22. Ahn, J.D., Dubern, B., Lubrano-Berthelier, C., Clement, K. & Karsenty, G. Cart overexpression is the only identifiable cause of high bone mass in melanocortin 4 receptor deficiency. *Endocrinology* **147**, 3196–3202 (2006).
23. Kalinova, J., Triska, J. & Vrchotova, N. Distribution of vitamin E, squalene, epicatechin, and rutin in common buckwheat plants (*Fagopyrum esculentum* Moench). *J. Agric. Food Chem.* **54**, 5330–5335 (2006).
24. Zeng, H. *et al.* Neuromedin U receptor 2–deficient mice display differential responses in sensory perception, stress, and feeding. *Mol. Cell. Biol.* **26**, 9352–9363 (2006).
25. Elias, C.F. *et al.* Leptin differentially regulates NPY and POMC neurons projecting to the lateral hypothalamic area. *Neuron* **23**, 775–786 (1999).
26. Graham, E.S. *et al.* Neuromedin U and Neuromedin U receptor-2 expression in the mouse and rat hypothalamus: effects of nutritional status. *J. Neurochem.* **87**, 1165–1173 (2003).
27. Paxinos, G. & Franklin, K. *The Mouse Brain in Stereotaxic Coordinates* 2nd edn. (Academic Press, San Diego, 2001).

Available online at www.sciencedirect.com
ScienceDirect
Journal of Steroid Biochemistry & Molecular Biology 103 (2007) 372–380
The Journal of Steroid Biochemistry & Molecular Biology
www.elsevier.com/locate/jsbmb

Ligand-induced transrepressive function of VDR requires a chromatin remodeling complex, WINAC

Shigeaki Kato[a,b,*], Ryoji Fujiki[a], Mi-Sun Kim[a], Hirochika Kitagawa[a]

[a] *The Institute of Molecular and Cellular Biosciences, The University of Tokyo, 1-1-1 Yayoi, Bunkyo-ku, Tokyo 113-0032, Japan*
[b] *ERATO, Japan Science and Technology Agency, Kawaguchi, Saitama 332-0012, Japan*

Received 30 November 2006

Abstract

We have previously shown that the novel ATP-dependent chromatin remodeling complex WINAC is required for the ligand-bound Vitamin D receptor (VDR)-mediated transrepression of the 25(OH)D_3 1α-hydroxylase [1α(OH)ase] gene. However, the molecular basis for VDR promoter association, which does not involve its binding to specific DNA sequences, remains unclear. To address this issue, we investigated the function of WSTF in terms of the association between WINAC and chromatin for ligand-induced transrepression by VDR. Results of *in vitro* experiments using chromatin templates showed that the association of unliganded VDR with the promoter required physical interactions between WSTF and both VDR and acetylated histones prior to VDR association with chromatin. The acetylated histone-interacting region of WSTF was mapped to the bromodomain, and a WSTF mutant lacking the bromodomain served as a dominant-negative mutant in terms of ligand-induced transrepression of the 1α(OH)ase gene. Thus, our findings indicate that WINAC associates with chromatin through a physical interaction between the WSTF bromodomain and acetylated histones, that appears to be indispensable for VDR/promoter association for ligand-induced transrepression of 1α(OH)ase gene expression.

Keywords: Acetylated histone; Transrepression; VDIR; VDR; WSTF

1. Introduction

Lipophilic ligands, such as fat-soluble Vitamins A and D, as well as thyroid/steroid hormones, are thought to exert their physiological effects through transcriptional control of target genes via cognate nuclear receptors (NRs) [1]. NRs form a gene superfamily, and they act as ligand-inducible activators. A number of co-regulator complexes that support ligand-dependent transcription control have been identified, and these complexes can be classified into three categories according to function [2]. The first co-regulator complex class regulates transcriptional control directly, through a physical interaction with general transcription factors and RNA polymerase II [3,4]. Members of the second co-regulator complex class modify histone tails covalently, for example by acetylation, in promoter nucleosomal arrays [5–8]. The major function of the last class of complexes is chromatin remodeling, which involves the ATP-dependent dynamic remodeling of chromatin structure [9–13]. Chromatin remodeling complexes utilize energy from ATP hydrolysis to rearrange nucleosomal arrays in a non-covalent manner. As chromosomal DNA is generally packed as nucleosomal arrays, chromatin remodeling complexes are thought to render specific promoter regions accessible to other co-regulator complex classes and sequence-specific regulators.

Recently, we identified a novel, multifunctional, ATP-dependent chromatin remodeling complex, designated WINAC, which consists of 13 subunits [11]. It contains SWI/SNF chromatin remodeling complex components and DNA replication-related factors. VDR interacts with WINAC in a ligand-independent manner through the Williams syndrome transcription factor (WSTF). WSTF contains a bromodomain that is adjacent to a zinc-finger motif of the

* Corresponding author at: The Institute of Molecular and Cellular Biosciences, The University of Tokyo, 1-1-1 Yayoi, Bunkyo-ku, Tokyo 113-0032, Japan. Tel.: +81 3 5841 8478; fax: +81 3 5841 8477.
E-mail address: uskato@mail.ecc.u-tokyo.ac.jp (S. Kato).

0960-0760/$ – see front matter © 2006 Elsevier Ltd. All rights reserved.
doi:10.1016/j.jsbmb.2006.12.038

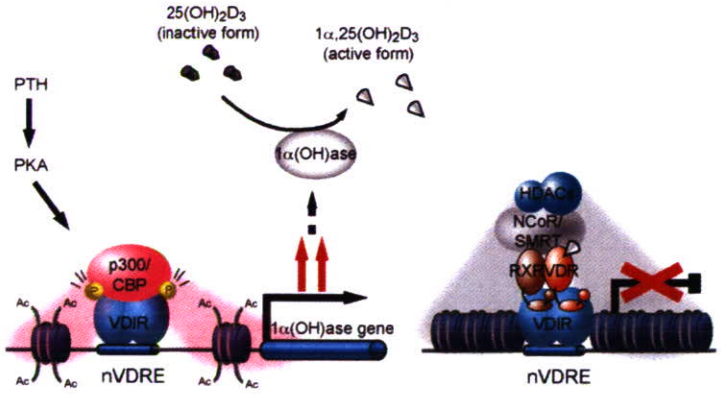

Fig. 1. Schematic view of ligand-induced transrepression by VDR in the human 1α(OH)ase gene promoter. A bHLH-type activator, VDIR, binds to the 1αnVDRE, and activates transcription. PKA signaling downstream of PTH/PTHrP phosphorylates VDIR, leading association of VDIR with HAT co-activator p300/CBP. Upon 1α,25(OH)$_2$D$_3$ binding, VDR associates with VDIR, inducing dissociation of the HAT co-activator, and recruitment of HDAC co-repressor for ligand-induced transrepression.

(BAZ) protein family. Members of this family harbor both a PHD finger and a bromodomain in their C-terminal domain [14]. As bromodomains have been recently shown to bind acetylated histones, it is possible that WSTF serves as an adaptor protein for acetylated histones, facilitating the association between WINAC and chromatin [15–18].

2. Vitamin D negatively regulates expression of the 25(OH)D$_3$ 1α-hydroxylase gene

Expression of the 25(OH)D$_3$ 1α-hydroxylase [1α(OH)ase] gene a key enzyme in Vitamin D biosynthesis, is negatively regulated by Vitamin D [19–21].

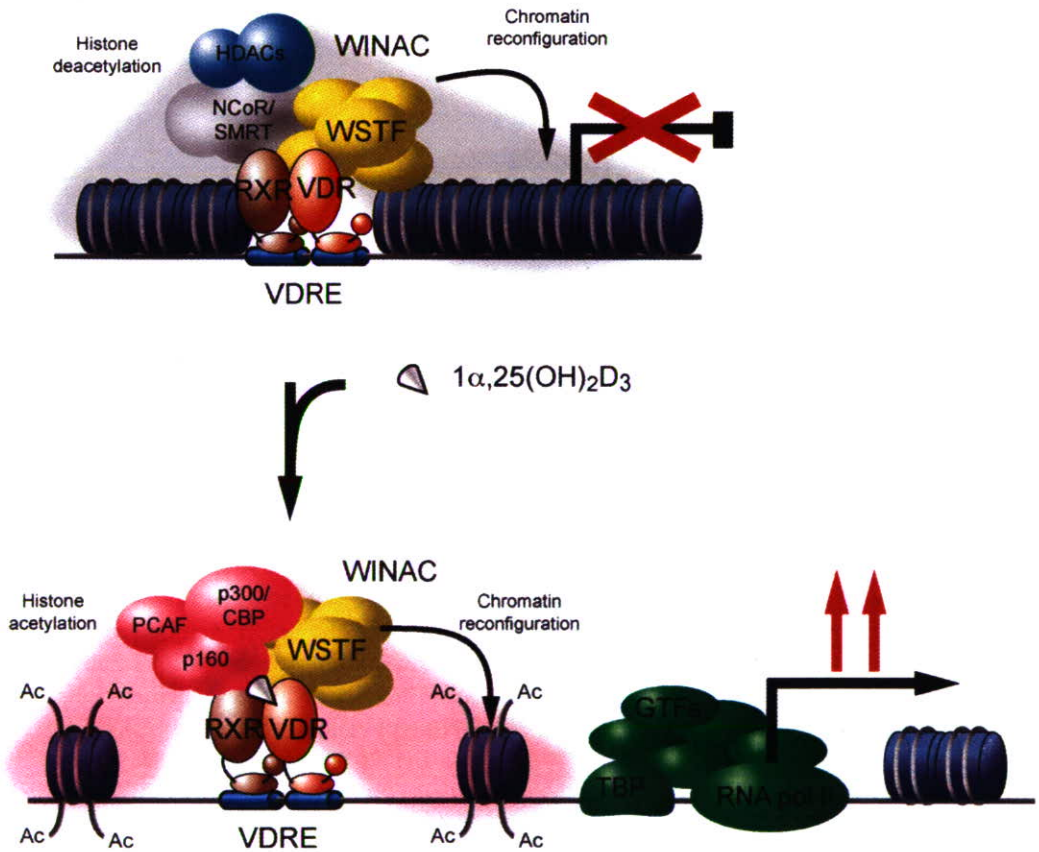

Fig. 2. WINAC supports ligand-induced transactivation by VDR. A WSTF-containing chromatin remodeling complex, WINAC, associates with VDR in a ligand-independent manner, and aids VDR to stably bind to the VDRE for ligand-induced transactivation.

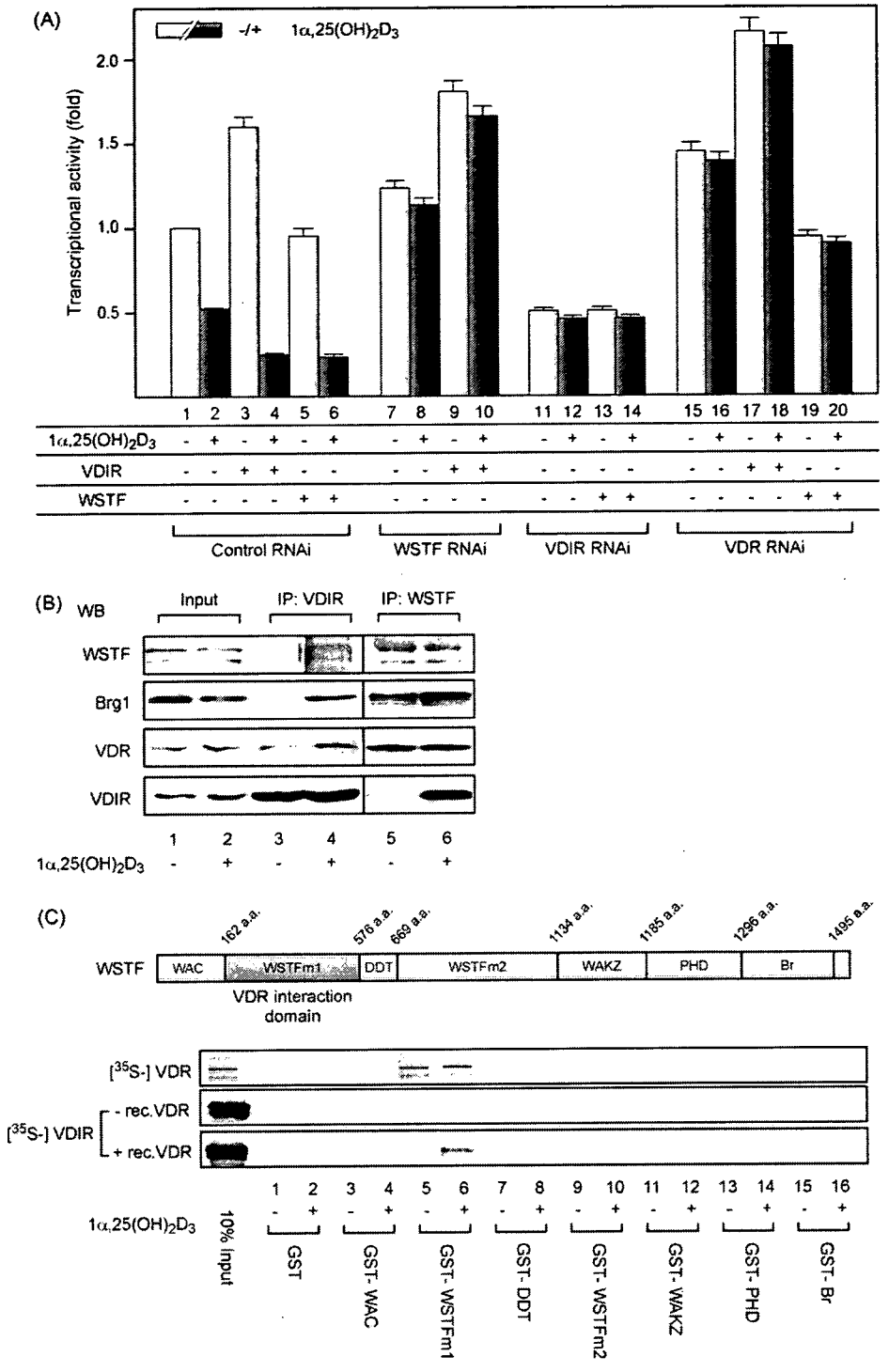

Fig. 3. WSTF enhances VDIR-mediated transrepression of 1α(OH)ase gene expression. (A) The effect of gene-specific knockdown of endogenous factors, WSTF, VDIR and VDR on 1α(OH)ase gene expression in a luciferase reporter assay. Gene-specific knockdown of the factors by RNAi was confirmed by Western blots using the relative antibodies (data not shown). MCF7 cells were transfected with 0.3 μg of the indicated siRNAs, 48 h after the transfection luciferase reporter gene containing 1α(OH)ase native promoter was transfected again into the cells. Luciferase activity was assessed after 12 h culture in the presence or absence of $1\alpha,25(OH)_2D_3$ (10^{-8} M). (B) $1\alpha,25(OH)_2D_3$-dependent interaction between endogenous WSTF and VDIR *in vivo*. MCF7 cells cultured with or without with $1\alpha,25(OH)_2D_3$ for 12 h were subjected to immunoprecipitation with anti-WSTF or anti-VDIR antibodies. Immunoprecipitates were Western blotted with specific antibodies as shown on the left. (C) SDS-PAGE gels of a series of GST-fused WSTF deletion mutants was visualized by CBB staining. Recombinant proteins were expressed in *E. coli* and purified by affinity chromatography. (D) GST pull-down assay. Schematic diagrams of the WSTF deletion mutants used are illustrated. [^{35}S]-labeled VDR translated *in vitro* was incubated with deletion mutants immobilized onto glutathione–sepharose beads in the presence or absence of $1\alpha,25(OH)_2D_3$ (10^{-6} M). Bound proteins were resolved by SDS-PAGE followed by autoradiography (upper panel). Autoradiographs show [^{35}S]-labeled VDIR, preincubated with (lower panel) or without (middle panel) cold recombinant VDR, bound to the GST-fused mutants immobilized on beads [22].

We recently reported that a bHLH-type activator, VDR-interacting repressor (VDIR), directly binds to the negative Vitamin D response element (1αnVDRE) in the human 1α(OH)ase gene promoter, thus activating transcription (Fig. 1) [22]. However, ligand-induced association between VDR and VDIR results in ligand-induced transrepression of 1α(OH)ase gene expression. This occurs through the switching of co-regulator complexes from histone acetyltransferase (HAT) co-activator complexes to histone deacetylase (HDAC) co-repressors upon VDIR binding to 1αnVDRE [22].

3. WSTF potentiates the ligand-induced transrepression by VDR in the human 1α(OH)ase gene promoter

We have previously shown that WINAC supports ligand-induced transactivation through chromatin remodeling [11] (see Fig. 2). However, it remained unclear if ligand-induced transrepression by VDR requires WINAC. To test this idea, the function of WSTF, with respect to ligand-induced VDR/VDIR transrepression, was studied by a transient expression assay using MCF7 cells, which express the 1α(OH)ase gene endogenously. A luciferase reporter gene plasmid containing two consensus 1αnVDRE sequences recognized by VDIR, that confer negative responsiveness to $1\alpha,25(OH)_2D_3$ in gene repression.

We found that endogenous VDR, VDIR and WSTF were responsible for ligand-induced negative responsiveness of the 1α(OH)ase gene, by their overexpression assay and RNAi approach (Fig. 3A). It is likely that WSTF mediates the ligand-induced transrepression of the 1α(OH)ase gene, together with VDR and VDIR.

We then examined the complex formed by these three factors in MCF-7 cells using an immunoprecipitation assay. As unliganded VDR was reported to associate with NCoR co-repressor complex [2], the co-repressor dissociation of exogenous VDR was observed in respond to ligand binding. As previously reported [11,22,23], while VDR associated with WSTF irrespective of $1\alpha,25(OH)_2D_3$ binding, $1\alpha,25(OH)_2D_3$ binding enhanced the interaction between VDR and VDIR (Fig. 3B).

By *in vitro* GST pull-down assay on a series of bacterially-expressed GST-fused WSTF mutants (Fig. 3C). The WSTF m1 domain (a.a. 163–576, illustrated as a shaded box above the panel) was found to interact with *in vitro* translated VDR, irrespective of $1\alpha,25(OH)_2D_3$ binding. While none of the WSTF regions exhibited physical interaction with VDIR, in the presence of $1\alpha,25(OH)_2D_3$-bound VDR, an association between WSTF and VDIR was detected (Fig. 3D, middle and lower panel). Together, these findings suggest that while WSTF interacts with VDR, VDIR is stably recruited only when VDR is liganded.

4. WSTF aids recruitment of ligand-unbound VDR to the 1α(OH)ase gene promoter

To test whether WSTF was recruited to VDIR via liganded VDR in the nuclei of living cells, we performed a ChIP assay using endogenous proteins and the native 1α(OH)ase gene promoter. In agreement with previous reports [11,22], VDIR was constitutively bound to 1αnVDRE (Fig. 4). As WSTF RNAi remarkably attenuated the promoter occupancy of VDR in the absence of ligand, WSTF appeared to facilitate the binding of ligand-unbound VDR to the 1αnVDRE region (Fig. 4).

To clarify the mechanism by which WSTF targets unliganded VDR to the promoter *in vitro*, we addressed which factors are indispensable for the promoter targeting of unliganded VDR by employing an immobilized DNA/chromatin template recruitment assay. DNA fragments containing either 1αnVDRE (−60 to −615) or the 1α(OH)ase distal region (−3632 to −3032) were end-biotinylated to allow their immobilization onto streptavidin beads. Using these factors, the end-biotinylated DNA fragments were correctly reconstituted into nucleosome arrays according to the MNase digestion assay (Fig. 5A). Whole cell extracts from MCF-7 cells that stably expressed FLAG-tagged WSTF treated

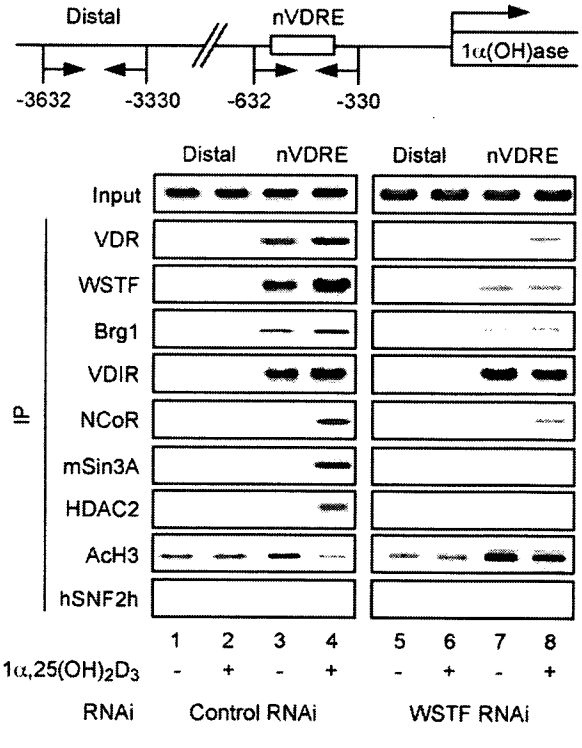

Fig. 4. WSTF is indispensable for ligand-induced promoter assembly of the VDR and HDAC co-repressor complex. Recruitment of VDR, WSTF, VDIR, and other co-regulators to the 1α(OH)ase gene promoter *in vivo*, as shown by ChIP analysis. Soluble chromatin was prepared from MCF7 cells treated with $1\alpha,25(OH)_2D_3$ (10^{-8} M) for 45 min and immunoprecipitated with the indicated antibodies. Extracted DNA samples were amplified using primer pairs that covered the 1α(OH)ase negative VDRE region (1αnVDRE) [11,22] or a distal region (3 kb upstream from 1αnVDRE) as a control.